



## Robust Multivariate Quantiles in Ranking Problems

Asmerilda Hitaj<sup>1</sup> · Elisa Mastrogiacomo<sup>1</sup> · Matteo Rocca<sup>1</sup> · Marco Tarsia<sup>1</sup>

Received: 17 April 2025 / Accepted: 20 October 2025  
© The Author(s) 2025

### Abstract

Multi-criteria decision-making is a valuable tool for evaluating and ranking alternatives with multiple conflicting criteria. Traditional methods assume precise inputs, which is rarely the case in practice. A recent approach tackles this using cumulative distribution functions and quantiles for multivariate random vectors, relying on cone-induced partial orders to build a conservative ranking procedure that reflects multiple expert opinions. Yet, expert weights and evaluations are often uncertain due to preferences, limited data, or subjective judgment. This paper extends the cone-based method to address both types of uncertainty. By modeling weights and evaluations as uncertain sets, we develop a dual-uncertainty framework to enhance decision robustness. We introduce robust versions of cone distribution functions and set-valued quantiles. Numerical examples illustrate how uncertainty affects rankings, offering a flexible tool for robust analysis in finance, sustainability planning, and public policy.

**Keywords** Multi-criteria decision-making · Set-valued functionals · Robust cone distribution functions · Robust set-quantile functions · Modeling under uncertainty · Decision robustness

---

✉ Marco Tarsia  
marco.tarsia@uninsubria.it

Asmerilda Hitaj  
asmerilda.hitaj@uninsubria.it

Elisa Mastrogiacomo  
elisa.mastrogiacomo@uninsubria.it

Matteo Rocca  
matteo.rocca@uninsubria.it

<sup>1</sup> University of Insubria, Varese, Italy

## 1 Introduction

Making informed decisions in the presence of multiple, often conflicting criteria is a central challenge in many fields. Multi-criteria decision-making (MCDM) offers a structured framework to tackle this complexity and plays a significant role in domains including economics, healthcare systems, infrastructure design, and environmental governance. Over the years, a variety of methods have been developed, ranging from classical deterministic models to more recent approaches that explicitly account for uncertainty and imprecision.

Classical MCDM methods, such as AHP, introduced by Saaty (1980), ELECTRE, developed by Roy (1968), and PROMETHEE, initially proposed by Mareschal et al. (1984) and later formalized and extended by Brans and Vincke (1985), rely on a fixed assignment of weights to criteria to rank alternatives. These deterministic approaches assume that decision-makers can express their preferences precisely, resulting in a single, fixed ranking of alternatives. For a comprehensive overview of different MCDM methods, see Belton and Stewart (2002) and Figueira et al. (2016). However, it is well-known that real-world decision-making often involves uncertainty arising from cognitive limitations, incomplete information, or subjective judgments.

To model such uncertainty, the seminal work of Bellman and Zadeh (1970) introduced fuzzy set theory as a formal framework for handling imprecise information, establishing the notion of decision-making in a *fuzzy environment*. This foundational contribution was later extended to multi-criteria problems by Carlsson (1982), who explored the integration of fuzzy set theory with MCDM techniques. Building on these early developments, Buckley (1984) proposed a fuzzy set approach to address the multiple-judge, multiple-criteria ranking problem, enabling aggregation of subjective judgments from different decision-makers. He further advanced the application of fuzzy logic in MCDM by introducing a method for ranking alternatives using fuzzy numbers in Buckley (1985b). Finally, in Buckley (1985a), a fuzzy extension of the AHP was developed, which allowed linguistic terms and fuzzy pairwise comparisons to be incorporated systematically into hierarchical decision structures.

Subsequent research has further enhanced the ability of MCDM models to handle uncertainty, particularly in group decision-making contexts where achieving consensus is challenging. For instance, fuzzy integrals, such as the Choquet integral, enable non-additive aggregation and can capture interaction effects among criteria. This approach was formalized by Grabisch (1996) and has been applied in various preference modeling settings.

Alongside fuzzy approaches, probabilistic methods have gained increasing attention. Techniques such as Monte Carlo simulation allow decision-makers to explore a range of weight configurations and preference profiles, producing probabilistic rankings that reflect uncertainty in input judgments; see Fu and Chang (2024). Interval-based methods, as discussed in Vahdani and Hadipour (2011), support the use of ranges rather than fixed values for weights and evaluations, thereby enabling more flexible assessments under uncertainty. These uncertainty-aware techniques have been successfully integrated into MCDM frameworks, enhancing significantly their capability to deal with imprecise or vague data; see, among others, Lahdelma et al.

(1998), Opricovic and Tzeng (2004), Lahdelma and Salminen (2010) and Corrente et al. (2014).

More recent contributions in robust MCDM aim to identify alternatives that perform consistently well across various scenarios. A key challenge is determining reliable criteria weights.

To address this, Danielson and Ekenberg (2017) introduces the CSR method, based on rank order and preference strength, showing stability in multi-stakeholder settings. Further advancements include a distributionally robust consensus model by Zhu et al. (2024), a robust minimum cost consensus model (RMCCM) by Zhang et al. (2022), and risk-based weighting via expected utility theory proposed by Liu (2024). Robust exploration in high-dimensional spaces is also supported through Markov-chain Monte Carlo techniques [see Fu and Chang (2024)]. These approaches demonstrate how robustness and risk sensitivity can be embedded in group and multi-criteria decision-making. A recent review [see Pajasmaa et al. (2024)] synthesizes the state-of-the-art, emphasizing the need for realistic validation and future studies on behavior and dynamic aggregation.

A significant advancement in MCDM is the integration of set-theoretic techniques, offering increased flexibility and robustness. The paper by Hamel and Kostner (2018) introduced a novel approach for ranking alternatives by evaluating them across possible importance directions provided by different judges, rather than using a single deterministic weight vector. This cone distribution function framework captures varying preferences, providing a more robust view of the decision space. It generates rankings that include non-convex regions of the Pareto frontier [see Kostner (2020)], enabling more granular decision-making through set-valued quantiles.

Building on Hamel and Kostner (2018) and Kostner (2020), this work incorporates two critical types of uncertainty: (1) uncertainty in the importance vectors assigned by judges, and (2) uncertainty in the criterion evaluations of alternatives. These reflect the complexities of real-world decision-making, where precise weightings and exact evaluations are often unrealistic. Judges may not be able to provide definitive weights due to imprecision in preferences, and evaluations often rely on incomplete or ambiguous data. By incorporating uncertainty into both weights and evaluations, our approach increases robustness and reduces sensitivity to small variations in input. This dual-uncertainty framework supports more realistic modeling by better capturing human variability and data imperfections. By adapting set optimization and cone distribution functions to this context, we produce rankings that reflect a broader range of scenarios. As a result, decision-makers are better equipped to make reliable and well-supported choices, even in highly uncertain environments.

The structure of the paper is as follows. Section 2 outlines key MCDM concepts, focusing on set optimization, cone distribution functions, and the role of uncertainty. Section 3 introduces the two types of uncertainties addressed. Sections 4 and 5 present our extended MCDM model, including, respectively, the robust cone distribution and quantile functions. Section 6 illustrates the methodology through a case study. Section 7 concludes and outlines future research directions.

## 2 Background

This section summarizes the approach introduced by Kostner (2020) in the context of MCDM, which builds on the cone distribution function and the set-valued upper and lower quantiles from Hamel and Kostner (2018). First, we recall the notions of *importance cone*,  $K_I$ , and *acceptance cone*,  $K_A$ . The *acceptance cone* is conceptually related to the solvency cone—an important construct from financial mathematics, whose geometric interpretation extends beyond that field; see Hamel and Heyde (2010). The former captures trade-offs among experts, while the latter represents the common region of acceptability, consisting of all alternatives that satisfy the judges' requirements. Second, we introduce the cone distribution function and set-valued quantiles from Hamel and Kostner (2018), and outline their role in decision-making.

### 2.1 Modeling Judges' Preferences

In MCDM, a set of  $m$  alternatives  $A = \{a_1, a_2, \dots, a_m\}$  is evaluated based on a set of  $d$  criteria  $\Gamma = \{\gamma_1, \gamma_2, \dots, \gamma_d\}$ . When  $n$  experts (advisors, judges) are involved in the generation of collective assessment, each judge  $J_j$ , for  $j = 1, \dots, n$ , provides an *importance vector*  $v^j : \Gamma \rightarrow \mathbb{R}_+^d \setminus \{0\}$ , which specifies the relative importance assigned to the different criteria:

$$v^j = \begin{bmatrix} v^j(\gamma_1) \\ \vdots \\ v^j(\gamma_d) \end{bmatrix}.$$

Each alternative  $a_i$ ,  $i = 1, \dots, m$  is evaluated by an external evaluator, resulting in a  $d$ -dimensional assessment vector:

$$x^E(a_i) = \begin{bmatrix} x^E(\gamma_1, a_i) \\ \vdots \\ x^E(\gamma_d, a_i) \end{bmatrix},$$

where the component  $x^E(\gamma_k, a_i)$  represents the score of the alternative  $a_i$  with respect to the criterion  $\gamma_k$ . The set of all evaluations is denoted by  $\mathcal{E} = \{x^E(a_1), \dots, x^E(a_m)\}$ .

The experts' weights can be aggregated according to a specific criterion for collective assessment. The approach proposed in Kostner (2020) uses the *importance cone*,  $K_I$ , defined as the convex cone generated by the judges' importance vectors:

$$K_I = \left\{ \sum_{j=1}^n \alpha_j v^j \mid \alpha_1, \dots, \alpha_n \geq 0 \right\}.$$

This cone represents all possible nonnegative combinations of the judges' preferences and captures potential compromises among them.

For each judge  $J_j$ ,  $j = 1, \dots, n$ , we can define a *half-space* of acceptable alternatives as:

$$H^+(v^j) := \{z \in \mathbb{R}^d | (v^j)^\top z \geq 0\},$$

that is, a vector  $z \in \mathbb{R}^d$  is deemed acceptable if, and only if,  $(v^j)^\top z \geq 0$ . Geometrically,  $H^+(v^j)$  corresponds to the closed half-space bounded by the hyperplane orthogonal to  $v^j$ , containing all directions forming a nonnegative angle with  $v^j$ . In other words, it represents the collection of “nonnegative” alternatives with respect to the importance vector  $v^j$ .

The intersection of the half-spaces  $H^+(v^j)$ ,  $j = 1, \dots, n$ ,

$$K_A = \bigcap_{j=1}^n H^+(v^j)$$

is called *acceptance cone*. It represents the region of alternatives that simultaneously satisfy the preferences of all judges. By the bipolar theorem [see, e.g., (Rockafellar 1970, Part III, Chapter 14, Theorem 14.5)], it follows that the importance cone  $K_I$  and the acceptance cone  $K_A$  are dual to each other.

**Example 1** To fix ideas, we consider a decision-making example with 3 criteria  $\gamma_i$ ,  $i = 1, 2, 3$ , and 3 judges. Suppose that the importance vectors of the judges are  $v^1 = [2, 1, 1]^\top$ ,  $v^2 = [1, 2, 1]^\top$ , and  $v^3 = [1, 1, 2]^\top$ . The resulting importance and acceptance cones are represented in Fig. 1.

## 2.2 Decision-Making by Cone Distribution Functions and Set-Quantiles

To address the ranking problem of the alternatives  $a_1, \dots, a_m$  under multiple-criteria using cone distribution functions and set-valued quantiles, we translate the decision-making process into a multivariate statistical framework. We construct a suitable probability space  $(\Omega, \mathcal{F}, \mathbb{P})$  as follows. We set  $\Omega = \{a_1, \dots, a_m\}$ ,  $\mathcal{F} = \mathcal{P}(\Omega)$ , and let  $\mathbb{P}$  be the uniform probability distribution on  $\Omega$ , i.e.,  $\mathbb{P}(a_i) = \frac{1}{m}$ ,  $i = 1, \dots, m$ . The evaluation of the alternatives under each criterion is summarized by a random vector  $X : \Omega \rightarrow \mathbb{R}^d$  defined as

$$X(a_i) = \begin{bmatrix} x^E(\gamma_1, a_i) \\ \vdots \\ x^E(\gamma_d, a_i) \end{bmatrix}, \quad i = 1, \dots, m.$$

Following (Kostner 2020), alternatives are ranked using cone distribution functions. For an importance vector  $v \in K_I \setminus \{0\}$ , the *scalar distribution function*  $F_{X,v} : \mathbb{R}^d \rightarrow [0, 1]$  is defined as:

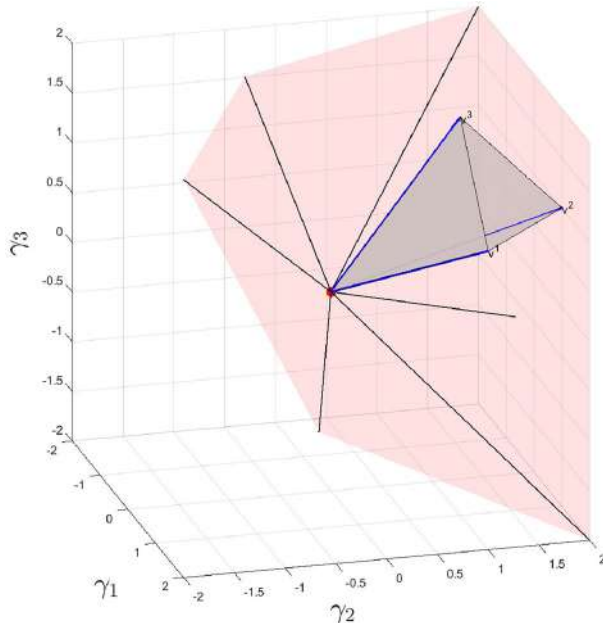


**Fig. 1** The light red region represents the acceptance cone  $K_A$ , while the shaded triangular region illustrates the importance cone  $K_I$ , both generated by the judges' importance vectors  $v^1 = [2, 1, 1]^\top$ ,  $v^2 = [1, 2, 1]^\top$ , and  $v^3 = [1, 1, 2]^\top$ , which are displayed as blue arrows

$$F_{X,v}(z) := \mathbb{P}(v^\top X \leq v^\top z), \quad (1)$$

that is,  $F_{X,v}$  is the cumulative distribution function of the discrete random variable  $v^\top X$ . More explicitly,

$$\begin{aligned} F_{X,v}(z) &= \mathbb{P}(v^\top X \leq v^\top z) \\ &= \frac{1}{m} \# \{i \in \{1, \dots, m\} \mid X(a_i) \in z - H^+(v)\} \\ &= \frac{1}{m} \# \{i \in \{1, \dots, m\} \mid x^E(a_i) \in z - H^+(v)\}. \end{aligned}$$

Hence, for  $z \in \mathbb{R}^d$ ,  $F_{X,v}$  measures the proportion of alternatives dominated by  $z$  along the direction induced by  $v$ .

The *cone distribution function*  $F_{X,K_A}(z)$  considers all possible directions within  $K_I$ , since

$$F_{X,K_A}(z) = \inf_{v \in K_I \setminus \{0\}} F_{X,v}(z), \quad (2)$$

and provides a conservative ranking based on the worst-case evaluation across the judges' preferences.  $F_{X,K_A}(z)$  enjoys several properties that admit interesting interpretations within the framework of MCDM. For a complete list, we refer to Kostner

(2020, Subsection 2.2). These properties make  $F_{X,K_A}(z)$  a suitable tool for ranking the alternatives  $a_1, \dots, a_m$  in the presence of multiple experts: the higher the value of  $F_{X,K_A}(x^E(a_i))$  in  $[0, 1]$ , the higher the position of  $a_i$  in the ranking. Alternatives with the same value of  $F_{X,K_A}$  are not comparable with respect to this ranking.

We observe that, when considering a single judge with a fixed importance vector  $v$ , the ranking method presented here corresponds to the *weighted sum method*, since each alternative  $a$  is evaluated through the scalar product  $(x^E(a))^\top v$ . This method has long been valued for its clarity and ease of use. Its linear structure makes it very intuitive: the criteria can be aggregated in a straightforward way, and the role of the weights is immediately visible and easy to explain. Due to these features, it has found wide application in practice. However, its weaknesses are equally well known, see among others Rowley et al. (2012) and the reference therein. The outcome of the method depends strongly on how the criteria are scaled or normalized, and even small changes in the assigned weights can significantly alter the ranking. In addition, the approach is fully compensatory: an alternative that performs poorly on one criterion may still appear favorable if it scores well on others. Finally, its linear formulation restricts the ability to represent more complex or nonlinear preference patterns, which may be essential in many real-world decision problems.

In contrast, the *cone distribution function* provides an aggregation method that not only incorporates the most extreme opinions among the judges, but also accounts for potential compromises across all judges. This aggregation is by construction nonlinear, owing to the presence of the infimum operator in Definition 2, which yields a more conservative and risk-averse ranking procedure. Indeed, the infimum of a sum is not, in general, equal to the sum of the respective infima.

**Example 2** Suppose that the set of alternatives consists of 5 elements, i.e.,  $A = \Omega = \{a_i\}_{i=1,\dots,5}$ , and that the criteria assessments are given by the following vectors:

$$\begin{aligned} x^E(a_1) &= [1, 5, 3]^\top, & x^E(a_2) &= [2, 3, 1]^\top, & x^E(a_3) &= [3, 2, 4]^\top, \\ x^E(a_4) &= [5, 1, 2]^\top, & x^E(a_5) &= [5, 5, 3]^\top, \end{aligned}$$

which are also illustrated in Fig. 2.

The five alternatives are ranked using the cone distribution function, along with the individual rankings corresponding to each judge, whose importance vectors were introduced in Example 1. These rankings are shown in Table 1.

By comparing the ranking derived from the cone distribution function  $F_{X,K_A}$  with those obtained from the “scalarized” distribution functions  $F_{X,v^j}$ , we observe that  $F_{X,K_A}$  always assigns lower values. This is simply because  $F_{X,K_A}$  is the infimum taken over all possible nonzero directions in  $K_I$ . Moreover,  $a_5$  is ranked first since  $x^E(a_5)$  is a non-dominated point among all alternatives (with respect to the cone  $K_I$ ). Finally, it is possible for different alternatives to share the same rank, meaning that they are indifferent with respect to the ranking induced by  $K_A$ .

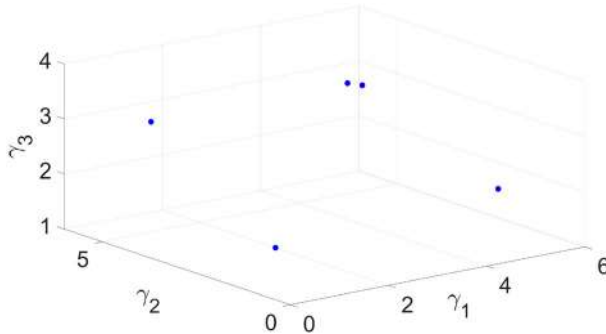


**Fig. 2** Evaluation of alternatives  $a_i, i = 1, \dots, 5$

### 2.3 Cone Quantiles

Set-valued quantiles for multivariate distributions with respect to a convex cone introduced in Hamel and Kostner (2018). For  $v \in K_A \setminus \{0\}$ , the lower  $v$ -quantile function of  $X$  is the set-valued function  $Q_{X,v}^- : ]0, 1[ \rightarrow \mathcal{P}(\mathbb{R}^d)$  defined as:

$$\begin{aligned} Q_{X,v}^-(p) &= \{z \in \mathbb{R}^d | F_{X,v}(z) \geq p\} \\ &= \left\{z \in \mathbb{R}^d \mid \#\{i \in \{1, \dots, m\} | x^E(a_i) \in z - H^+(v)\} \geq mp\right\}. \end{aligned} \quad (3)$$

The set  $Q_{X,v}^-(p)$  includes all points  $z \in \mathbb{R}^d$ , such that, with probability at least  $p$ , the inequality  $X^\top v \leq z^\top v$  holds.

The *lower  $K_A$ -quantile* function of  $X$  is defined as the intersection of the lower  $v$ -quantiles over all non-zero elements of  $K_I$ , i.e., as the set-valued function  $Q_{X,K_A}^- : ]0, 1[ \rightarrow \mathcal{P}(\mathbb{R}^d)$  given by

$$Q_{X,K_A}^-(p) = \bigcap_{v \in K_I \setminus \{0\}} Q_{X,v}^-(p). \quad (4)$$

The set  $Q_{X,K_A}^-(p)$  contains all points  $z \in \mathbb{R}^d$  such that, with probability at least  $p$ , the vector  $X$  is “less than or equal to”  $z$  according to the preorder induced by the acceptance cone  $K_A$ . Similarly, the set-valued function  $Q_{X,v}^+ : ]0, 1[ \rightarrow \mathcal{P}(\mathbb{R}^d)$  is defined as:

$$Q_{X,v}^+(p) = \left\{z \in \mathbb{R}^d \mid \#\{i \in \{1, \dots, m\} | x^E(a_i) \in z - \text{int } H^+(v)\} \leq mp\right\}, \quad (5)$$

and is called upper  $v$ -quantile function of  $X$ . The *upper cone quantile*  $Q_{X,K_A}^+(p)$  is then defined as:

$$Q_{X,K_A}^+(p) = \bigcap_{v \in K_I \setminus \{0\}} Q_{X,v}^+(p). \quad (6)$$

**Table 1** Rankings based on  $F_{X,K_A}$  and  $F_{X,v^j}$  for  $j = 1, 2, 3$ , with corresponding ranks shown in parentheses

$z = x^E(a_i)$	$F_{X,K_A}(z)$	$F_{X,v^1}(z)$	$F_{X,v^2}(z)$	$F_{X,v^3}(z)$
$a_1$	0.4 (2)	0.4 (4)	0.8 (2)	0.6 (3)
$a_2$	0.2 (5)	0.2 (5)	0.4 (4)	0.2 (5)
$a_3$	0.4 (2)	0.6 (3)	0.6 (3)	0.8 (2)
$a_4$	0.4 (2)	0.8 (2)	0.4 (4)	0.4 (4)
$a_5$	1 (1)	1 (1)	1 (1)	1 (1)

In a MCDM setting, these quantile functions allow us to classify alternatives into “good” and “bad” regions relative to a threshold  $p \in ]0, 1[$ . The lower cone quantile  $Q_{X, K_A}^-(p)$  identifies alternatives ranked at least as high as  $p$ , while the upper cone quantile  $Q_{X, K_A}^+(p)$  identifies those ranked at most as high as  $p$ . Alternatively, quantiles can define an ordinal preference scale  $\mathcal{G}$ , e.g., {very low, low, medium, high, very high}, where each level corresponds to a probability interval. A typical partition of the unit interval is  $\mathcal{I} = \{[0, 0.2[, [0.2, 0.4[, [0.4, 0.6], [0.6, 0.8[, [0.8, 1]\}$ . For instance, alternatives in  $Q_{X, K_A}^+(0.2)$  are “very low”, those in  $Q_{X, K_A}^+(0.4) \setminus Q_{X, K_A}^+(0.2)$  are “low”, and so on.

Set-valued quantiles have useful properties for decision-making, including affine equivariance, monotonicity, conservatism, right-continuity, and robustness. For a detailed discussion of these properties, we refer to Hamel and Kostner (2018) and Kostner (2020), and to the analysis presented below concerning the robust counterpart of set-quantiles.

**Example 3** *Figure 3 illustrates the lower and upper  $K_A$ -quantiles for various  $p$  values, in the setting of Examples 1 and 2. Note that  $Q_{X, K_A}^-(p) \cap Q_{X, K_A}^+(p)$  may be empty or non-empty depending on the data and the value of  $p$ .*

### 3 Introducing Uncertainty

In the original formulation by Kostner (2020), the importance vectors  $v^j$ , for  $j = 1, \dots, n$ , represent fixed judgments on the relative significance of criteria, and alternative evaluations are assumed to be precise. However, in real-world contexts, such assumptions often fail: judges may not know exact weights, and evaluations may be imprecise due to limited data or differing interpretations. To address these issues, we extend the framework in Kostner (2020) by incorporating uncertainty into both the importance vectors and the criterion evaluations. This leads to a more realistic representation of preferences and improves the robustness of the decision-making process. We now introduce several ways to model uncertainty—both in forming the importance cone and in evaluating alternatives—highlighting that different choices are possible and offer a flexible toolkit for practical applications.

#### 3.1 Uncertainty in the Importance Vector of Each Judge

Experts in real-world settings may be unable to assign exact, fixed weights to each criterion. To model this uncertainty, we introduce variability in the importance vectors by considering a set of possible importance cones.

Formally, the original importance cone  $K_I$  is associated with a set of perturbed cones:

$$K_I^{(S)} := \{K_I^s \mid s \in S\},$$

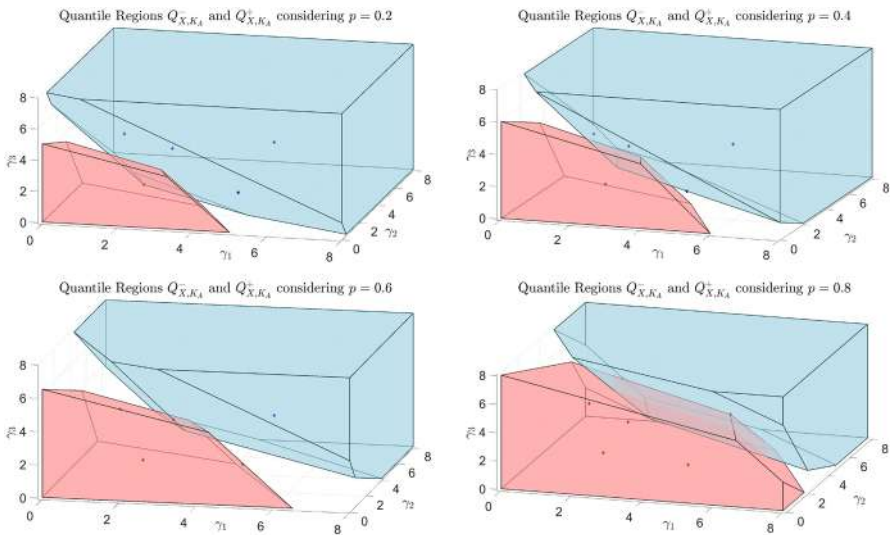


**Fig. 3** The set  $Q_{X,K_A}^-(p)$  is shown in blue and the set  $Q_{X,K_A}^+(p)$  in light red, for  $p = 0.2, 0.4, 0.6, 0.8$ . The importance cone  $K_A$  is generated by the judges' vectors  $v^1, v^2$ , and  $v^3$

called *set of uncertain cones*. Each  $K_I^s$ , for  $s \in S$ , corresponds to a scenario generated from a set of perturbed importance vectors  $(v^{j,s})_{s \in S} \subset \mathbb{R}_+^d \setminus \{0\}$ . Specifically, for each  $s \in S$ , we define:

$$K_I^s = \left\{ \sum_{j=1}^n \alpha_j v^{j,s} \mid \alpha_1, \dots, \alpha_n \geq 0 \right\}.$$

One of the reasons for the use of the perturbed cones is that each expert may not be willing or be able to provide exact values of his weights. This difficulty could be avoided by allowing the experts to give some variability in their own weights. The set  $S$  is used here to indexing the set of uncertain importance cones and may be finite, countable, or uncountable. For instance, if we assume that the set of uncertain importance cones is finite,  $S$  could be chosen as  $S = \{1, \dots, S\}$  with  $K_I^{(S)} = \{K_I^1, \dots, K_I^S\}$ . In case we assume a countable number of uncertain vectors  $S$  could be chosen as  $S = \mathbb{N}$ , so that the set of uncertain importance cones can be described through a sequence of cones  $K_I^{(S)} = \{K_I^s\}_{s \in \mathbb{N}}$ . Finally, if we want to introduce an uncountable uncertainty set, a possible choice for  $S$  could be  $S = [0, 1]$  so that the uncertainty set of importance vectors becomes  $K_I^{(S)} = \{K_I^s\}_{s \in [0,1]}$ . Figure 4 shows an example with six uncertain cones surrounding the original cone  $K_I$  from Example 1. Another possibility is to allow the variability of the weights for each expert  $j$ , for instance, through small deviations around a fixed vector of weights  $v^j$ ; in this case the perturbed importance vectors can be assumed to belong to the closed balls in  $\mathbb{R}^d$  centered at  $v^j$ , i.e.,  $v^{j,s} \in B_\varepsilon(v^j)$ . However, one could even assign a

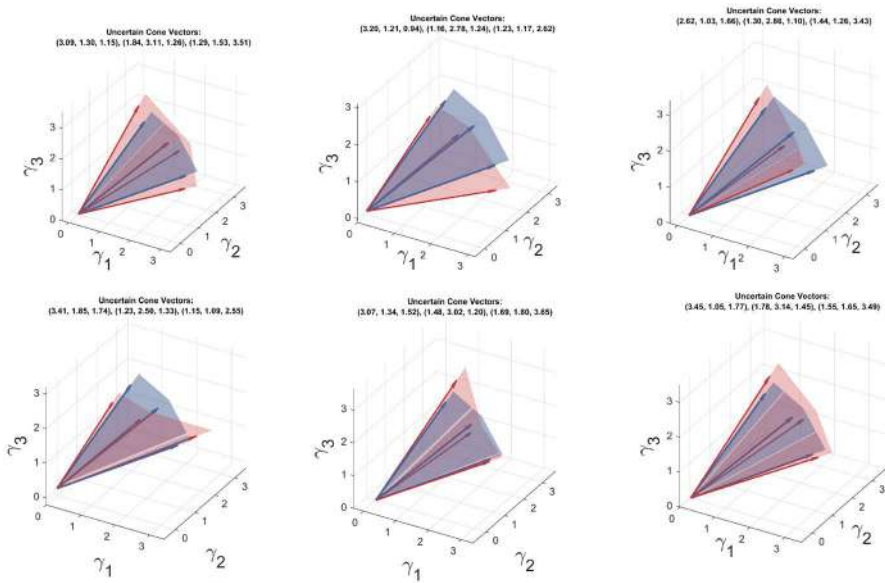


**Fig. 4** Each subplot displays the original cone (in blue) alongside one instance of an uncertain cone (in red) within a three-dimensional criterion space. The original cone is generated by the three importance vectors of Example 1. The uncertain cones illustrate possible deviations caused by uncertainty in these vectors, with the specific vectors forming each uncertain cone indicated in the title of each subplot. This depiction highlights the range of potential configurations under uncertainty, showing how the judges' importance vectors might shift

probability distribution over  $S$  to reflect how likely each cone  $K_I^s$  is (such extensions could be explored in future research).

Depending on the uncertainty level, the perturbed cones may expand beyond or shrink within  $K_I$ . This formulation captures the range of plausible expert judgments and enhances the flexibility and robustness of the MCDM framework.

### 3.2 Uncertainty in Criteria Evaluation of Alternatives

The accuracy of alternative evaluations is another key source of uncertainty in MCDM. Each alternative  $a_i$  is initially assessed by a fixed evaluation vector provided by an external evaluator:

$$x^E(a_i) = \begin{bmatrix} x^E(\gamma_1, a_i) \\ x^E(\gamma_2, a_i) \\ \vdots \\ x^E(\gamma_d, a_i) \end{bmatrix} \in \mathbb{R}^d,$$

where  $x^E(\gamma_k, a_i)$  is the score of  $a_i$  under criterion  $\gamma_k$ . Since these scores are often estimates, it is important to account for possible inaccuracies due to limited data,

subjective interpretation, or incomplete information—similar to the uncertainty considered for importance vectors.

To model this, we associate the evaluation set  $X$  with an uncertainty set  $\mathcal{U}_X$ , containing  $X$ , which captures potential perturbations. A common choice for  $\mathcal{U}_X$  is a closed ball centered at  $X$  with radius  $\varepsilon$ , defined under a suitable distance metric. The selected metric determines the shape and size of the uncertainty region. Figure 5 illustrates four different metrics, each inducing a distinct uncertainty set:

- (i) The  $L_2$ -norm (*Euclidean distance*)—the simplest and most intuitive example—assumes uniform uncertainty in all directions:

$$\mathcal{U}_X := \left\{ X' : \Omega \rightarrow \mathbb{R}^d \mid \sqrt{\sum_{k=1}^d |X'(\gamma_k, a_i) - X(\gamma_k, a_i)|^2} \leq \varepsilon, \forall i = 1, \dots, m \right\},$$

where  $X'(\gamma_k, a_i)$  indicates the perturbed point. This choice is appropriate when each criterion is subject to the same degree of uncertainty.

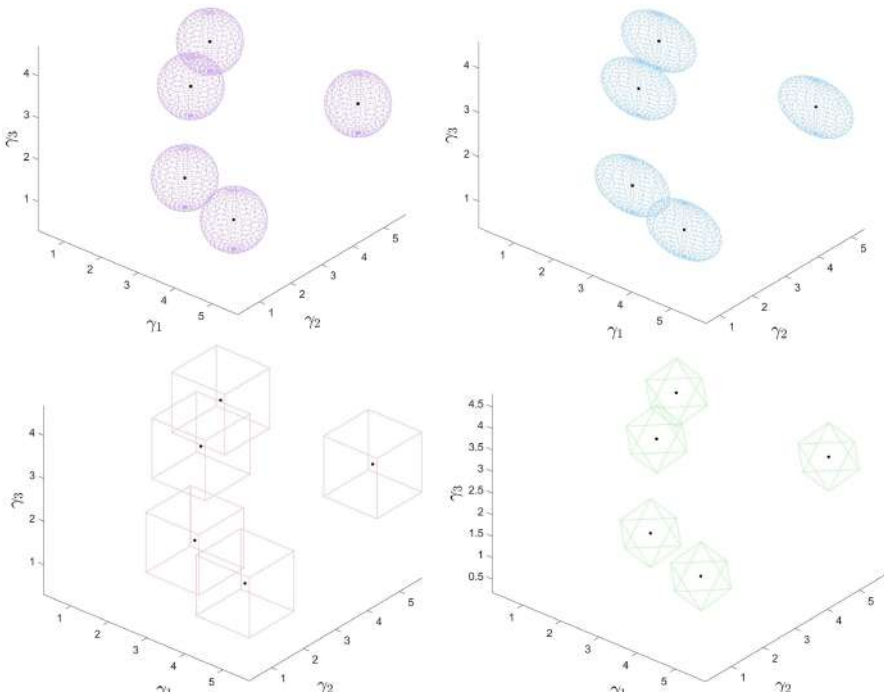


**Fig. 5** Examples of uncertainty sets for criteria evaluations: The four subplots illustrate different shapes of uncertainty sets around each point  $x^E(a_i)$ . Each subplot corresponds to a distinct metric: (Top Left)  $L_2$ -norm: circular uncertainty (light purple); (Top Right) Mahalanobis distance: ellipsoidal uncertainty (light blue); (Bottom Left)  $L_\infty$ -norm: square uncertainty (light red); (Bottom Right)  $L_1$ -norm: diamond-shaped uncertainty (light green). These sets capture regions where the evaluation of each alternative is considered uncertain

- (ii) The *Mahalanobis distance* accounts for the variance and correlation structure among the criteria, leading to ellipsoidal uncertainty regions:

$$\mathcal{U}_X := \left\{ X' : \Omega \rightarrow \mathbb{R}^d \mid \sqrt{\sum_{k,\ell=1}^d \theta_{k,\ell} (X'(\gamma_k, a_i) - X(\gamma_k, a_i)) (X'(\gamma_\ell, a_i) - X(\gamma_\ell, a_i))} \leq \varepsilon, \forall i = 1, \dots, m \right\}$$

where  $\theta_{k,\ell}$ ,  $k, \ell = 1, \dots, d$  are the entries of a symmetric positive definite matrix that determines the shape and size of the ellipsoidal region.

- (iii) The  $L_\infty$ -norm (*Chebyshev distance*) defines distance based on the maximum deviation along any single criterion:

$$\mathcal{U}_X := \left\{ X' : \Omega \rightarrow \mathbb{R}^d \mid \max_{k=1, \dots, d} |X'(\gamma_k, a_i) - X(\gamma_k, a_i)| \leq \varepsilon, \forall i = 1, \dots, m \right\},$$

resulting in a cubic uncertainty region.

- (iv) The  $L_1$ -norm (*Manhattan distance*) considers the sum of absolute deviations across all criteria:

$$\mathcal{U}_X := \left\{ X' : \Omega \rightarrow \mathbb{R}^d \mid \sum_{k=1}^d |X'(\gamma_k, a_i) - X(\gamma_k, a_i)| \leq \varepsilon, \forall i = 1, \dots, m \right\},$$

producing a diamond-shaped uncertainty region, suitable when cumulative deviations are more relevant than individual ones.

More advanced approaches involve using probabilistic distances between random vectors, such as the *Wasserstein distance* or the *Kullback–Leibler divergence*. These metrics allow one to quantify how different two  $d$ -dimensional probability distributions are, thus capturing not only geometric perturbations but also potential likelihood levels within the uncertainty set  $\mathcal{U}_X$ .

This allows decision-makers to consider a wider range of possible deviations from initial evaluations, enhancing the robustness of the analysis. Uncertainty in evaluations can also be combined with uncertainty in the importance vectors, resulting in a ranking problem with dual variability. In the next sections, we develop a framework that integrates both types of uncertainty.

## 4 Robust Cone Distribution Functions

In this section, we present the mathematical foundation for robust cone distribution functions, offering a rigorous framework to address uncertainty in both importance vectors and criterion evaluations. This approach enhances the reliability of decision-making by embedding uncertainty directly into the ranking and classification of alternatives. We also discuss key properties, including affine equivariance and monotonicity, to highlight the robustness and practical relevance of these functions in multi-criteria settings.

#### 4.1 Definitions

Let  $\mathcal{U}_X$  represent the uncertainty set for the evaluations of a random vector  $X$ . The acceptance cone  $K_A^s$ , for a given  $s \in S$ , is defined as the intersection of half-spaces determined by the uncertain importance vectors  $v_j^s$  for each judge  $j = 1, \dots, n$ :

$$K_A^s \doteq \bigcap_{j=1}^n H^+(v_j^s),$$

where  $H^+(v_j^s) = \left\{ z \in \mathbb{R}^d \mid (v_j^s)^\top z \geq 0 \right\}$ .

We define the two classes:

$$K_I^{(S)} := \{K_I^s \mid s \in S\}, \quad K_A^{(S)} := \{K_A^s \mid s \in S\} \quad (7)$$

representing all possible cones of importance and acceptance, respectively. For each  $s \in S$ , the cones  $K_I^s$  and  $K_A^s$  are dual, as shown in Kostner (2020).

We further define:

$$K_A^S \doteq \bigcap_{s \in S} K_A^s \quad (8)$$

which is a closed, convex cone in  $\mathbb{R}^d$ , with  $\mathbb{R}_+^d \subseteq K_A^S \subseteq \mathbb{R}^d$ .

Now, for any random vector  $X$ , we define the *robust cone distribution function*

$$F_{\mathcal{U}_X, K_A^{(S)}} : \mathbb{R}^d \rightarrow [0, 1],$$

or *robust  $K_A^{(S)}$ -distribution function (robust CDF)*, by setting, for any  $z \in \mathbb{R}^d$ ,

$$F_{\mathcal{U}_X, K_A^{(S)}}(z) \stackrel{\text{def}}{=} \inf_{s \in S, X' \in \mathcal{U}_X} F_{X', K_A^s}(z) \quad (9)$$

(see also (1) and (2)).

The intersection in (8) ensures that the robust acceptance cone captures the worst-case importance directions from the set  $S$ . Incorporating *importance vector uncertainty*  $s \in S$  in (9) guarantees robustness by accounting for all plausible expert assessments. Likewise, *criteria evaluation uncertainty*  $X' \in \mathcal{U}_X$  models variability in evaluations, further strengthening the robustness of the framework.

As already noted in Section 2, the ranking method based on the scalar distribution function coincides with the weighted sum method. However, the robust approach proposed in this section extends beyond the weighted sum formulation through the explicit incorporation of uncertainty. Unlike the non-robust case introduced in Kostner (2020), this distinction arises even when using the scalar distribution function, which corresponds to the single-expert scenario. In fact, if  $K_A^s$  reduces to a single vector  $v_s$  for all  $s \in S$ , then the scalar distribution function is replaced by

$$F_{\mathcal{U}_X, v^{(S)}}(z) := \inf_{s \in S, X' \in \mathcal{U}_X} F_{X', v^s}(z).$$

This expression introduces a nonlinearity in the ranking procedure due to the presence of the infimum operator.

**Remark 1** We conceive the definition (9) as extendable to a general family of closed and convex cones

$$C^{(S)} := \{C^s \mid s \in S\}$$

in  $\mathbb{R}^d$ . Specifically, for any random vector  $X$ , we mean as defined, for any  $z \in \mathbb{R}^d$ ,

$$F_{\mathcal{U}_X, C^{(S)}}(z) \doteq \inf_{s \in S, X' \in \mathcal{U}_X} F_{X', C^s}(z) \quad (10)$$

where, for any  $s \in S$ ,  $X' \in \mathcal{U}_X$ , and  $z \in \mathbb{R}^d$ ,

$$F_{X', C^s}(z) \doteq \inf_{v \in (C^s)^* \setminus \{0\}} F_{X', v}(p)$$

for  $F_{X', v}(p)$  being defined as in (1). In this context, for any random vector  $X$ , a closed and convex cone  $C$ , and any  $z \in \mathbb{R}^d$ , we introduce the following notations:

$$F_{\mathcal{U}_X, C}(z) \doteq \inf_{X' \in \mathcal{U}_X} F_{X', C}(z), \quad (11)$$

$$F_{X, C^{(S)}}(z) \doteq \inf_{s \in S} F_{X, C^s}(z). \quad (12)$$

Therefore, also by (10), on  $\mathbb{R}^d$ ,

$$F_{\{X\}, \{C\}} = F_{\{X\}, C} = F_{X, \{C\}} = F_{X, C}.$$

**Remark 2** A natural comparison arises between the robust CDF introduced here with the CDF in the sense of Hamel and Kostner, which take  $K_A^S$  as the reference acceptance cone (see (8)). Accordingly, we establish that, for any  $z \in \mathbb{R}^d$ ,

$$F_{\mathcal{U}_X, K_A^{(S)}}(z) \geq \inf_{X' \in \mathcal{U}_X} F_{X', K_A^S}(z). \quad (13)$$

The relation (13) influences the final ranking of alternatives.

This observation will be further supported by the numerical analysis in the following sections.

To prove (13), we first remember that, by (9) and (2), for any  $z \in \mathbb{R}^d$ ,

$$\begin{aligned} F_{\mathcal{U}_X, K_A^{(S)}}(z) &\equiv \inf_{s \in S, X' \in \mathcal{U}_X} F_{X', K_A^s}(z) \\ &= \inf_{s \in S, X' \in \mathcal{U}_X} \inf_{v \in K_I^s \setminus \{0\}} F_{X', v}(z) \end{aligned}$$

and, for any  $X' \in \mathcal{U}_X$ ,

$$F_{X', K_A^S}(z) = \inf_{v' \in \bigcup_{s' \in S} K_I^{s'} \setminus \{0\}} F_{X', v'}(z).$$

We also use that, by (8),

$$(K_A^S)^* = \bigcup_{s' \in S} K_I^{s'}.$$

It follows that, for any  $s \in S$  and  $v \in K_I^s \setminus \{0\}$ , we have that, for any  $X' \in \mathcal{U}_X$  and  $z \in \mathbb{R}^d$ ,

$$F_{X', v}(z) \geq F_{X', K_A^S}(z).$$

Then, for any  $s \in S$ ,  $X' \in \mathcal{U}_X$ , and  $z \in \mathbb{R}^d$ ,

$$F_{X', K_A^s}(z) \geq F_{X', K_A^S}(z),$$

and hence easily the thesis.

## 4.2 Properties

We present and prove several key properties of the robust cone distribution function  $F_{\mathcal{U}_X, K_A^{(S)}}(\cdot)$  for any random vector  $X$  (see (9)), which also depends on the structure of the corresponding neighborhood  $\mathcal{U}_X$ . These properties are particularly relevant for MCDM problems.

Throughout this paper, we write  $U \sim V$  to denote that random vectors  $U$  and  $V$  share the same joint distribution.

(*F-lawinv*) — law invariance: for any random vector  $Y$ , if  $X \sim Y$  and

$$\begin{cases} \forall X' \in \mathcal{U}_X, \exists Y' \in \mathcal{U}_Y : X' \sim Y' \\ \forall Y'' \in \mathcal{U}_Y, \exists X'' \in \mathcal{U}_X : X'' \sim Y'' \end{cases} \quad (14)$$

then, for any  $z \in \mathbb{R}^d$ ,

$$F_{\mathcal{U}_X, K_A^{(S)}}(z) = F_{\mathcal{U}_Y, K_A^{(S)}}(z). \quad (15)$$

This property ensures that  $F_{\mathcal{U}_X, K_A^{(S)}}(z)$  depends only on the distribution of  $X$ , rather than its specific realizations. This means that if two random vectors  $X$  and  $Y$  share the same distribution ( $X \sim Y$ ), the robust cone distribution function will produce identical results for both. The condition stated in (14) guarantees that the uncertainty sets  $\mathcal{U}_X$  and  $\mathcal{U}_Y$  preserve the law-equivalence structure, allowing to extend this invariance under uncertainty. Consequently, the equality in (15) holds for any  $z \in \mathbb{R}^d$ , meaning that  $X$  and  $Y$  are interchangeable from the perspective of the robust cone framework.

By focusing on the law of  $X$ , decision-makers ensure that the method remains consistent and fair regardless of the specific realizations of uncertain criteria evaluations. We now prove that, for any random vector  $X$ ,  $F_{\mathcal{U}_X, K_A^{(S)}}(\cdot)$  satisfies (F-lawinv). Let  $X$  and  $Y$  be two random vectors with  $X \sim Y$  and, for any  $X' \in \mathcal{U}_X$ , let  $Y' \in \mathcal{U}_Y$  be such that  $X' \sim Y'$ , according to the first line in (14). Then, by (1), (2) and (9), we have that, for any  $s \in S$  and  $z \in \mathbb{R}^a$ ,

$$F_{X', K_A^{(S)}}(z) = F_{Y', K_A^{(S)}}(z) \geq F_{\mathcal{U}_Y, K_A^{(S)}}(z)$$

and consequently, for any  $z \in \mathbb{R}^a$ ,

$$F_{\mathcal{U}_X, K_A^{(S)}}(z) \geq F_{\mathcal{U}_Y, K_A^{(S)}}(z).$$

The converse follows in a similar way, which allows us to obtain (15).

Let us present the first non-trivial property of the CDF.

(F-affequ) — *affine equivariance*: if  $b \in \mathbb{R}^d$  and  $B \in \mathbb{R}^{d \times d}$  is an invertible matrix such that

$$\mathcal{U}_{BX+b} = B\mathcal{U}_X + b \quad (16)$$

then, for any  $z \in \mathbb{R}^d$ ,

$$F_{\mathcal{U}_{BX+b}, BK_A^{(S)}}(Bz + b) = F_{\mathcal{U}_X, K_A^{(S)}}(z), \quad (17)$$

where the robust cone distribution function  $F_{\mathcal{U}, BK_A^{(S)}}(\cdot)$ , under any choice of uncertainty set  $\mathcal{U}$  modeling the imprecision in criteria evaluations, corresponds to the family of cones

$$BK_A^{(S)} := \{BK_A^s \mid s \in S\} \quad (18)$$

as outlined in Remark 1. This property ensures that  $F_{\mathcal{U}_X, K_A^{(S)}}$  remains invariant under affine transformations (translations and linear transformations) of the input data. This guarantees that the function behaves consistently regardless of changes in scale, units, or coordinate systems. It preserves the relative rankings of alternatives and maintains the geometric structure of the acceptance cone. As a result, this property improves the robustness, clarity, and reliability of the function in MCDM under uncertainty.

**Proposition 1** *For any random vector  $X$ , the robust cone distribution function  $F_{\mathcal{U}_X, K_A^{(S)}}(\cdot)$  satisfies (F-affequ).*

**Proof** Let  $X$  be an arbitrary random vector, and let  $b \in \mathbb{R}^d$  and  $B \in \mathbb{R}^{d \times d}$  be an invertible matrix. Based on Hamel and Kostner (2018), we can assert that, for any  $s \in S$ ,  $X' \in \mathcal{U}_X$  and  $z \in \mathbb{R}^a$ ,

$$F_{BX'+b, BK_A^s}(Bz + b) = F_{X', K_A^s}(z).$$

Therefore, by (9), (16) and Remark 1, we conclude that, for any  $z \in \mathbb{R}^d$ ,

$$\begin{aligned} F_{\mathcal{U}_X, K_A^{(S)}}(z) &= \inf_{s \in S, X' \in \mathcal{U}_X} F_{BX'+b, BK_A^s}(Bz + b) \\ &= \inf_{s \in S, Z' \in \mathcal{U}_{BX+b}} F_{Z', BK_A^s}(Bz + b) \\ &\equiv F_{\mathcal{U}_{BX+b}, BK_A^{(S)}}(Bz + b) \end{aligned}$$

as stated in (17) (see also (18)).  $\square$

We now turn to the various monotonicity properties of the CDF.

**(F-nondec)** — *monotone non-decreasing* (w.r.t.  $z$ ): for any  $z, z' \in \mathbb{R}^d$ , if  $z \leq_{K_A^S} z'$ , then

$$F_{\mathcal{U}_X, K_A^{(S)}}(z) \leq F_{\mathcal{U}_X, K_A^{(S)}}(z').$$

This property guarantees that  $F_{\mathcal{U}_X, K_A^{(S)}}(z)$  respects the partial order induced by  $K_A^S$ .

This ensures that alternatives performing better with respect to the acceptance cone structure receive higher or equal values, reinforcing the consistency of the ranking.

**(F-noninc)** — *monotone non-increasing* (w.r.t.  $K_A^S$ -order): for any random vector  $Y$ , if  $X \leq_{K_A^S} Y$  (a.s.) and

$$\forall X' \in \mathcal{U}_X, \exists Y' \in \mathcal{U}_Y : X' \leq_{K_A^S} Y' \text{ a.s.} \quad (19)$$

then, for any  $z \in \mathbb{R}^d$ ,

$$F_{\mathcal{U}_Y, K_A^{(S)}}(z) \leq F_{\mathcal{U}_X, K_A^{(S)}}(z). \quad (20)$$

This property highlights the behavior of the robust cone distribution function under order-preserving transformations. If a random vector  $X$  performs at least as well as  $Y$  in the sense of the cone  $K_A^S$ , then the robust cone distribution function of  $X$  will dominate that of  $Y$ . This property ensures that alternatives demonstrating stronger performance relative to the cone structure receive lower or equal values, aligning with a worst-case evaluation perspective.

**(F-cmon)** — *cone monotonicity*: for any family  $C_A^{(S)} := \{C_A^s \mid s \in S\}$  of closed and convex cones in  $\mathbb{R}^d$ , if, for any  $s \in S$ ,  $\mathbb{R}_+^d \subseteq C_A^s \subseteq \mathbb{R}^d$  and

$$\forall s \in S, \exists \bar{s} \in S : C_A^{\bar{s}} \subseteq K_A^s \quad (21)$$

then, for any  $z \in \mathbb{R}^d$ ,

$$F_{\mathcal{U}_X, C_A^{(S)}}(z) \leq F_{\mathcal{U}_X, K_A^S}(z) \quad (22)$$

(see Remark 1). This property highlights the relationship between two families of cones,  $C_A^{(S)}$  and  $K_A^S$ . If (21) is true, then the robust cone distribution function evaluated with  $C_A^{(S)}$  will always yield values less than or equal to those obtained with  $K_A^S$ . This reflects the fact that narrower cones  $C_A^{(S)}$  impose stricter constraints on the feasible directions of importance, leading to a more restrictive and potentially less optimistic evaluation of the distribution function. This property is useful for comparing solutions under different levels of conservatism and for understanding the effects of tightening or relaxing the set of acceptable importance directions.

**Proposition 2** *For any random vector  $X$ , the robust cone distribution function  $F_{\mathcal{U}_X, K_A^S}(\cdot)$  satisfies the following monotonicity properties: (F-nondec), (F-noninc), (F-cmon).*

In the following, we prove the three properties stated above.

**Proof (F-nondec).** Let  $X$  be an arbitrary random vector, and let  $z, z' \in \mathbb{R}^d$  be such that  $z \leq_{K_A^S} z'$ , i.e., for any  $s \in S$ ,  $z \leq_{K_A^s} z'$  (see (8)). Then, by (9) and Hamel and Kostner (2018), it holds that, for any  $s \in S$  and  $X' \in \mathcal{U}_X$ ,

$$F_{\mathcal{U}_X, K_A^S}(z) \leq F_{X', K_A^s}(z) \leq F_{X', K_A^s}(z').$$

Thus, the thesis arises from the arbitrariness of  $X' \in \mathcal{U}_X$  and  $s \in S$ .

**(F-noninc).** Let  $X$  and  $Y$  be two random vectors with  $X \leq_{K_A^S} Y$  (a.s.) and, for any  $X' \in \mathcal{U}_X$ , let  $Y' \in \mathcal{U}_Y$  be such that  $X' \leq_{K_A^S} Y'$  (a.s.), as in (19). Then, by (8), for any  $s \in S$ ,  $X' \leq_{K_A^s} Y'$  (a.s.) and, by (9) and Hamel and Kostner (2018), we have that, for any  $z \in \mathbb{R}^d$ ,

$$F_{\mathcal{U}_Y, K_A^S}(z) \leq F_{Y', K_A^s}(z) \leq F_{X', K_A^s}(z),$$

from which (20) follows immediately.

**(F-cmon).** Let  $X$  be an arbitrary random vector and, for any  $s \in S$ , let  $C_A^s$  be a closed and convex cone with  $\mathbb{R}_+^d \subseteq C_A^s \subseteq \mathbb{R}^d$ . From (9), (21) and Hamel and Kostner (2018), we readily infer that, for any  $s \in S$ , there exists  $\bar{s} \in S$  such that, for any  $X' \in \mathcal{U}_X$  and  $z \in \mathbb{R}^d$ ,

$$F_{\mathcal{U}_X, C_A^{(S)}}(z) \leq F_{X', C_A^{\bar{s}}}(z) \leq F_{X', K_A^s}(z).$$

The inequality (22) is now a clear outcome. □

We conclude this subsection by addressing a noteworthy form of continuity of the CDF.

(F-rcont) — right continuity: for any  $\bar{z} \in \mathbb{R}^d$  and sequence  $(z_n)_{n \in \mathbb{N}}$  in  $\mathbb{R}^d$  with  $z_{n+1} \leq_{K_A^S} z_n$ ,  $n \in \mathbb{N}$ , if  $\lim_{n \rightarrow \infty} z_n = \bar{z}$ , then

$$\lim_{n \rightarrow \infty} F_{\mathcal{U}_X, K_A^{(S)}}(z_n) = \inf_{n \in \mathbb{N}} F_{\mathcal{U}_X, K_A^{(S)}}(z_n) = F_{\mathcal{U}_X, K_A^{(S)}}(\bar{z}).$$

This property ensures the stability of the robust cone distribution function when evaluated along a monotone decreasing sequence of points  $\{z_n\}$  in the cone order  $K_A^S$ . Specifically, as the sequence  $z_n$  converges to a limit point  $\bar{z}$ , the values of the robust cone distribution function converge to its value at  $\bar{z}$ . This property guarantees consistency and smooth behavior of the function under limits, which is crucial for theoretical soundness and numerical applications where approximations or iterative methods are used.

**Proposition 3** For any random vector  $X$ , the robust cone distribution function  $F_{\mathcal{U}_X, K_A^{(S)}}(\cdot)$  satisfies (F-rcont).

**Proof** Let  $X$  be an arbitrary random vector, and let  $\bar{z} \in \mathbb{R}^d$  and  $(z_n)_{n \in \mathbb{N}}$  be a sequence in  $\mathbb{R}^d$  such that, for any  $n \in \mathbb{N}$ ,  $z_{n+1} \leq_{K_A^S} z_n$ , i.e., for any  $s \in S$ ,  $z_{n+1} \leq_{K_A^s} z_n$  (see (8)). Given that  $\lim_{n \rightarrow \infty} z_n = \bar{z}$ , it results from Hamel and Kostner (2018) that, for any  $s \in S$  and  $X' \in \mathcal{U}_X$ ,

$$\lim_{n \rightarrow \infty} F_{X', K_A^s}(z_n) = \inf_{n \in \mathbb{N}} F_{X', K_A^s}(z_n) = F_{X', K_A^s}(\bar{z}). \quad (23)$$

Therefore, by (9),

$$\inf_{s \in S, X' \in \mathcal{U}_X} \inf_{n \in \mathbb{N}} F_{X', K_A^s}(z_n) = F_{\mathcal{U}_X, K_A^{(S)}}(\bar{z})$$

and in particular, for any  $s \in S$ ,  $X' \in \mathcal{U}_X$  and  $n \in \mathbb{N}$ ,

$$F_{\mathcal{U}_X, K_A^{(S)}}(\bar{z}) \leq F_{X', K_A^s}(z_n).$$

This fact immediately implies the inequality

$$\inf_{n \in \mathbb{N}} F_{\mathcal{U}_X, K_A^{(S)}}(z_n) \equiv \inf_{n \in \mathbb{N}} \inf_{s \in S, X' \in \mathcal{U}_X} F_{X', K_A^s}(z_n) \geq F_{\mathcal{U}_X, K_A^{(S)}}(\bar{z})$$

(see (9) again). Conversely, taking into account that, for any  $\bar{s} \in S$ ,  $\bar{X}' \in \mathcal{U}_X$  and  $n \in \mathbb{N}$ ,

$$F_{\mathcal{U}_X, K_A^{(S)}}(z_n) \equiv \inf_{s \in S, X' \in \mathcal{U}_X} F_{X', K_A^s}(z_n) \leq F_{\bar{X}', K_A^{\bar{s}}}(z_n)$$

it can be written, by (23), that, for any  $\bar{s} \in S$  and  $\bar{X}' \in \mathcal{U}_X$ ,

$$\inf_{n \in \mathbb{N}} F_{\mathcal{U}_X, K_A^{(S)}}(z_n) \leq \inf_{n \in \mathbb{N}} F_{\bar{X}', K_A^{\bar{s}}}(z_n) = F_{\bar{X}', K_A^{\bar{s}}}(\bar{z}).$$

This provides a clear conclusion to the proof.  $\square$

**Remark 3** Clearly, condition (21) is stronger than having the inclusion

$$C_A^S := \bigcap_{s \in S} C_A^s \subseteq K_A^S$$

(see (8)), without being equivalent in general.

**Remark 4** A widely discussed property of MCDM aggregation rules is independence of irrelevant alternatives (IIA). This principle states that the preference between any two alternatives should depend only on the evaluations of those two alternatives, and not be influenced by the presence or absence of other, irrelevant options. As discussed in the literature (see, among others, Dias et al. (2019)), this property is closely related to the rank reversal problem. This issue arises when, for example,  $z$  is preferred to  $y$ , and  $y$  is preferred to  $w$ , but removing  $w$  or adding a new alternative  $u$  may lead to the conclusion that  $y$  is preferred to  $z$ . Such behavior violates IIA. For the ranking method based on cone distribution functions, (Hamel and Kostner 2024, Section 4) analyzes the conditions under which rank reversal may occur and illustrates them with an example. Consequently, rank reversal may also arise in the robust version proposed in this paper.

## 5 Robust Cone Quantile Functions

In this section, we define the notion of robust set-valued quantiles and discuss their properties, following an approach analogous to that of the previous section.

### 5.1 Definitions

For any random vector  $X$ , we define the (set-valued) *robust lower cone quantile function*

$$Q_{\mathcal{U}_X, K_A^{(S)}}^- : ]0, 1[ \rightarrow \mathcal{P}(\mathbb{R}^d),$$

or *robust lower  $K_A^{(S)}$ -quantile function (lower CQF)*, by setting, for any  $p \in ]0, 1[$ ,

$$Q_{\mathcal{U}_X, K_A^{(S)}}^-(p) \stackrel{\text{def}}{=} \bigcap_{s \in S, X' \in \mathcal{U}_X} Q_{X', K_A^s}^-(p) \quad (24)$$

where, for any  $s \in S$  and  $X' \in \mathcal{U}_X$ ,  $Q_{X', K_A^s}^-(\cdot)$  is the lower  $K_A^{(S)}$ -quantile function à la (Hamel and Kostner 2018) (see (4)). Here,  $\mathcal{P}(\mathbb{R}^d)$  denotes the power set of  $\mathbb{R}^d$ . Observe that, by (4), (2), and (9),

$$\begin{aligned}
Q_{\mathcal{U}_X, K_A^{(S)}}^-(p) &= \bigcap_{s \in S, X' \in \mathcal{U}_X} \left\{ z \in \mathbb{R}^d \mid F_{X', K_A^s}(z) \geq p \right\} \\
&= \left\{ z \in \mathbb{R}^d \mid F_{\mathcal{U}_X, K_A^{(S)}}(z) \geq p \right\} \\
&= (F_{\mathcal{U}_X, K_A^{(S)}})^{-1}([p, 1]). 
\end{aligned} \tag{25}$$

Likewise, for any random vector  $X$ , we define the (set-valued) *robust upper cone quantile function*

$$Q_{\mathcal{U}_X, K_A^{(S)}}^+ : ]0, 1[ \rightarrow \mathcal{P}(\mathbb{R}^d),$$

or *robust upper  $K_A^{(S)}$ -quantile function (upper CQF)*, by setting, for any  $p \in ]0, 1[,$

$$Q_{\mathcal{U}_X, K_A^{(S)}}^+(p) \stackrel{\text{def}}{=} \bigcap_{s \in S, X' \in \mathcal{U}_X} Q_{X', K_A^s}^+(p) \tag{26}$$

where, for any  $s \in S$  and  $X' \in \mathcal{U}_X$ ,  $Q_{X', K_A^s}^+(\cdot)$  is the upper  $K_A^{(S)}$ -quantile function (see (6)).

**Remark 5** In accordance with Remark 1, Definitions (25) and (24) may also be naturally interpreted within the framework of a broad class of closed and convex cones  $C^{(S)} = \{C^s \mid s \in S\}$  in  $\mathbb{R}^d$ : for any random vector  $X$  and  $p \in ]0, 1[,$

$$Q_{\mathcal{U}_X, C^{(S)}}^-(p) \doteq \bigcap_{s \in S, X' \in \mathcal{U}_X} Q_{X', C^s}^-(p) \tag{27}$$

and

$$Q_{\mathcal{U}_X, C^{(S)}}^+(p) \doteq \bigcap_{s \in S, X' \in \mathcal{U}_X} Q_{X', C^s}^+(p),$$

where, for any  $s \in S$ ,  $X' \in \mathcal{U}_X$ , and  $p \in ]0, 1[,$

$$Q_{X', C^s}^\pm(p) \doteq \bigcap_{v \in (C^s)^* \setminus \{0\}} Q_{X', v}^\pm(p),$$

for  $Q_{X', v}^\pm(p)$  being defined as in (3) and (5) respectively. Observe that, as per (25),

$$Q_{\mathcal{U}_X, C^{(S)}}^-(p) = (F_{\mathcal{U}_X, C^{(S)}})^{-1}([p, 1])$$

(see Remark 1). In this context, for any random vector  $X$ , a closed and convex cone  $C$ , and any  $p \in ]0, 1[, we introduce the following notations:$

$$Q_{\mathcal{U}_X, C}^-(p) \doteq \bigcap_{X' \in \mathcal{U}_X} Q_{X', C}^-(p), \quad (28)$$

$$Q_{X, C^{(S)}}^-(p) \doteq \bigcap_{s \in S} Q_{X, C^s}^-(p).$$

In particular, also by (27), on  $]0, 1[$ ,

$$Q_{\{X\}, \{C\}}^-=Q_{\{X\}, C}^-=Q_{X, \{C\}}^-=Q_{X, C}^-.$$

**Remark 6** Following the line of discussion in Remark 2, we can now compare the robust CQFs and the CQFs corresponding to  $K_A^S$ . What emerges is that, for any  $p \in ]0, 1[$ ,

$$\bigcap_{X' \in \mathcal{U}_X} Q_{X', K_A^S}^-(p) \subseteq Q_{\mathcal{U}_X, K_A^{(S)}}^-(p). \quad (29)$$

This aspect will be clearly illustrated in the upcoming application section.

To verify the set inclusion above, let us recall that, by (25), for any  $p \in ]0, 1[$ ,

$$Q_{\mathcal{U}_X, K_A^{(S)}}^-(p) = \left\{ z \in \mathbb{R}^d \mid F_{\mathcal{U}_X, K_A^{(S)}}(z) \geq p \right\}$$

and, by definitions, for any  $X' \in \mathcal{U}_X$ ,

$$Q_{X', K_A^S}^-(p) = \left\{ z \in \mathbb{R}^d \mid F_{X', K_A^S}(z) \geq p \right\}.$$

Then, clearly,

$$\bigcap_{X' \in \mathcal{U}_X} Q_{X', K_A^S}^-(p) = \left\{ z \in \mathbb{R}^d \mid \inf_{X' \in \mathcal{U}_X} F_{X', K_A^S}(z) \geq p \right\},$$

and, therefore, the claim is directly obtained by (13) (Remark 2).

We now present the basic properties of  $Q_{\mathcal{U}_X, K_A^{(S)}}^-(\cdot)$ , with these conditions being fundamentally based on the propositions of the previous subsection. The analogous properties of  $Q_{\mathcal{U}_X, K_A^{(S)}}^+(\cdot)$  follow in a similar manner. Please refer to Remark 1 also for further context.

**Remark 7** We firstly highlight that, for any  $p \in ]0, 1[$ ,  $Q_{\mathcal{U}_X, K_A^{(S)}}^-(p)$  is a closed, convex and  $\leq_{K_A^S}$ -upper closed subset of  $\mathbb{R}^d$ . In particular, for any  $p \in ]0, 1[$ ,

$$Q_{\mathcal{U}_X, K_A^{(S)}}^-(p) \oplus K_A^S = Q_{\mathcal{U}_X, K_A^{(S)}}^-(p).$$

*Closure ensures stability under limits, which is essential for both theoretical analysis and numerical implementation. Convexity reflects risk aversion, ensuring that convex combinations of quantiles remain within the acceptance set, in line with coherent risk principles. The upper closure property with respect to  $K_A^S$  (see (8)) implies that, if a point belongs to the CQF, then all points above it in the cone order do as well. These properties provide a solid mathematical framework for applications in financial engineering, decision analysis, and multi-criteria optimization, ensuring both analytical rigor and computational feasibility.*

To ascertain the properties above, let  $X$  be an arbitrary random vector. For any  $s \in S$  and  $X' \in \mathcal{U}_X$ , the lower  $K_A^{(S)}$ -quantile function  $Q_{X', K_A^s}^-(\cdot)$  is such that, for any  $p \in ]0, 1[$ ,  $Q_{X', K_A^s}^-(p)$  is a closed, convex and  $\leq_{K_A^s}$ -upper closed subset of  $\mathbb{R}^d$ , as established in Hamel and Kostner (2018). Hence, for any  $p \in ]0, 1[$ , the set  $Q_{\mathcal{U}_X, K_A^{(S)}}^-(p)$ , which, by (25), is the intersection over  $s \in S$  and  $X' \in \mathcal{U}_X$  of the sets  $Q_{X', K_A^s}^-(p)$ , is itself closed, convex and  $\leq_{K_A^s}$ -upper closed in  $\mathbb{R}^d$  (see also (8)). Finally, observe that, for any  $p \in ]0, 1[$ , the identity

$$Q_{\mathcal{U}_X, K_A^{(S)}}^-(p) \oplus K_A^S = Q_{\mathcal{U}_X, K_A^{(S)}}^-(p)$$

i.e., the inclusion  $\subseteq$  (since  $0 \in K_A^S$ ), is equivalent to the fact that  $Q_{\mathcal{U}_X, K_A^{(S)}}^-(p)$  is  $\leq_{K_A^s}$ -upper closed (meaning precisely that, for any  $z, z' \in \mathbb{R}^d$ , if  $z \in Q_{\mathcal{U}_X, K_A^{(S)}}^-(p)$  and  $z \leq_{K_A^s} z'$ , then  $z' \in Q_{\mathcal{U}_X, K_A^{(S)}}^-(p)$  as well).

## 5.2 Properties

Let us begin by discussing the properties of the (lower) CQF.

(*Q*-lawinv) — law invariance: for any random vector  $Y$ , if  $X \sim Y$  and (14) holds, then, for any  $p \in ]0, 1[$ ,

$$Q_{\mathcal{U}_X, K_A^{(S)}}^-(p) = Q_{\mathcal{U}_Y, K_A^{(S)}}^-(p).$$

This property ensures that the CQF depends only on the distribution of the random variable and not on specific realizations.

It is easy to verify that, for any random vector  $X$ ,  $Q_{\mathcal{U}_X, K_A^{(S)}}^-(\cdot)$  satisfies (*Q*-lawinv). Indeed, let  $X$  and  $Y$  be two random vectors with  $X \sim Y$ . Since (14) holds, (15) follows as a consequence: that is,

$$F_{\mathcal{U}_X, K_A^{(S)}} = F_{\mathcal{U}_Y, K_A^{(S)}}$$

on  $\mathbb{R}^d$  (see (*F*-lawinv)). From this and (25), the thesis is directly derived.

Let's turn to a more significant property.

**( $\mathcal{Q}$ -affequ)** — *affine equivariance*: if  $b \in \mathbb{R}^d$  and  $B \in \mathbb{R}^{d \times d}$  is an invertible matrix such that (16) holds, then, for any  $p \in ]0, 1[$ ,

$$Q_{\mathcal{U}_{Bx+b}, BK_A^{(S)}}^-(p) = BQ_{\mathcal{U}_x, K_A^{(S)}}^-(p) + b$$

(see Remark 5 and (18)). This property ensures that the CQFs behave coherently under such transformations: a shift in location translates into an identical shift in the quantile function, while a linear transformation of risk factors modifies the CQFs accordingly. In practice, this means that CQFs remain meaningful under changes of scale or shifts in the reference frame, ensuring stability when modeling risks across different markets and portfolio structures. Affine transformations play a crucial role in convex analysis, with applications ranging from optimization and decision sciences to financial modeling and related fields.

**Proposition 4** *For any random vector  $X$ , the robust lower  $K_A^{(S)}$ -quantile function  $Q_{\mathcal{U}_x, K_A^{(S)}}^-(\cdot)$  satisfies ( $\mathcal{Q}$ -affequ).*

**Proof** Let  $X$  be an arbitrary random vector, and let  $b \in \mathbb{R}^d$  and  $B \in \mathbb{R}^{d \times d}$  be an invertible matrix such that (16) is fulfilled. Then, for any  $z, z' \in \mathbb{R}^d$  such that  $z = Bz' + b$ , or equivalently  $z' = B^{-1}(z - b)$ , (17) results in

$$F_{\mathcal{U}_{Bx+b}, BK_A^{(S)}}(z) = F_{\mathcal{U}_x, K_A^{(S)}}(z')$$

(see ( $F$ -affequ), and in particular (18) and Remark 1). Therefore, by (25) and Remark 5, we find that, for any  $p \in ]0, 1[$ ,

$$\begin{aligned} Q_{\mathcal{U}_{Bx+b}, BK_A^{(S)}}^-(p) &\equiv \left\{ z \in \mathbb{R}^d \mid F_{\mathcal{U}_{Bx+b}, BK_A^{(S)}}(z) \geq p \right\} \\ &= B \left\{ z' \in \mathbb{R}^d \mid F_{\mathcal{U}_x, K_A^{(S)}}(z') \geq p \right\} + b \\ &\equiv BQ_{\mathcal{U}_x, K_A^{(S)}}^-(p) + b, \end{aligned}$$

as asserted. □

We now proceed to examine the different monotonicity properties of the CQF.

**( $\mathcal{Q}$ -pmon)** —  *$p$ -monotonicity*: for any  $p, p' \in ]0, 1[$ , if  $p \leq p'$ , then

$$Q_{\mathcal{U}_x, K_A^{(S)}}^-(p') \subseteq Q_{\mathcal{U}_x, K_A^{(S)}}^-(p).$$

This property states that as we move toward higher probability levels, the associated CQF shrinks or remains unchanged. Essentially, the worst-case scenarios covered by the quantile function become less severe as we move to higher percentiles, aligning with coherent risk assessment principles. For instance, in financial risk management,

this reflects the idea that higher confidence levels should correspond to increasingly conservative risk estimates.

(*Q*-noninc) — *monotone non-increasing* (w.r.t.  $K_A^S$ - order): for any random vector  $Y$ , if  $X \leq_{K_A^S} Y$  (a.s.) and (19) holds, then, for any  $p \in ]0, 1[$ ,

$$Q_{\mathcal{U}_Y, K_A^{(S)}}^-(p) \subseteq Q_{\mathcal{U}_X, K_A^{(S)}}^-(p).$$

If one random variable is always at least as large as another in the partial order induced by the acceptance cone  $K_A^S$ , then its CQF must be at least as conservative. This property is crucial in systemic risk modeling , and more generally in robust decision-making and stochastic optimization, where dependencies or comparisons under a partial order must preserve the consistency of rankings.

(*Q*-cmon) — *cone monotonicity*: for any class  $C_A^{(S)} := \{C_A^s \mid s \in S\}$  of closed and convex cones in  $\mathbb{R}^d$  such that, for any  $s \in S$ ,  $\mathbb{R}_+^d \subseteq C_A^s \subseteq \mathbb{R}^d$ , if (21) holds, then, for any  $p \in ]0, 1[$ ,

$$Q_{\mathcal{U}_X, C_A^{(S)}}^-(p) \subseteq Q_{\mathcal{U}_X, K_A^{(S)}}^-(p)$$

(see Remark 5). This property ensures that whenever we transition between acceptance cones in a structured manner, the corresponding CQFs adjust coherently. This is particularly relevant in multi-asset risk assessments, where different assets or portfolios may be evaluated under different acceptance criteria due to regulatory or institutional constraints. More generally, when risk measures are defined over cone -valued sets of risk factors, it is essential that the quantile structure respects the hierarchy of acceptance sets.

**Proposition 5** *For any random vector  $X$ , the robust lower  $K_A^{(S)}$ - quantile function  $Q_{\mathcal{U}_X, K_A^{(S)}}^-(\cdot)$  satisfies the following monotonicity properties: (*Q*-pmon), (*Q*-noninc), (*Q*-cmon).*

In the following, we prove the three properties stated above.

**Proof (*Q*-pmon).** Let  $X$  be an arbitrary random vector, and let  $p, p' \in ]0, 1[$  be such that  $p \leq p'$ . Hence, by (25), for any  $z \in \mathbb{R}^d$ , if  $F_{\mathcal{U}_X, K_A^{(S)}}(z) \geq p'$  (i.e.,  $z \in Q_{\mathcal{U}_X, K_A^{(S)}}^-(p')$ ), then, a fortiori,  $F_{\mathcal{U}_X, K_A^{(S)}}(z) \geq p$  (i.e.,  $z \in Q_{\mathcal{U}_X, K_A^{(S)}}^-(p)$ ), which is exactly as claimed.

**(*Q*-noninc).** Let  $X$  and  $Y$  be two random vectors such that  $X \leq_{K_A^S} Y$  (a.s.), and assume (19). Then, (20) is satisfied, namely,

$$F_{\mathcal{U}_Y, K_A^{(S)}} \leq F_{\mathcal{U}_X, K_A^{(S)}}$$

on  $\mathbb{R}^d$  (see (*F*-noninc)). Thus, the thesis is immediately obtained (see (25)).

(*Q*-cmon). Let  $X$  be an arbitrary random vector and, for any  $s \in S$ , let  $C_A^s$  be a closed and convex cone with  $\mathbb{R}_+^d \subseteq C_A^s \subseteq \mathbb{R}^d$ . By virtue of (21), (22) holds true: on  $\mathbb{R}^d$ ,

$$F_{\mathcal{U}_X, C_A^{(S)}} \leq F_{\mathcal{U}_X, K_A^{(S)}}$$

(see (*F*-cmon)). The desired conclusion is easily reached.  $\square$

**Remark 8** First-order stochastic dominance (FSD) provides a way to compare random variables based on their cumulative distribution functions. In the univariate case, a random variable  $X$  is said to dominate another random variable  $Y$  in the sense of FSD if, and only if, their cumulative distribution functions satisfy  $F_X(t) \leq F_Y(t)$  for all  $t \in \mathbb{R}$ . This condition ensures that  $X$  yields outcomes that are, in a probabilistic sense, at least as favorable as those of  $Y$ .

In a structured setting, where dependencies and constraints shape the space of admissible random variables, this principle extends naturally through a cone-based formulation. Here, ordering relations are influenced by regulatory, portfolio, or market-driven criteria, allowing for a refined comparison of random elements in a multi-dimensional space. In this framework, given any random vector  $Y$ , we write

$$X \leq_{FSD}^{wc} Y$$

(*wc* stands for worst-case) to denote the generalized form of first-order stochastic dominance w.r.t. the cone  $K_A^S$ . Specifically, for any  $z \in \mathbb{R}^d$ ,

$$F_{\mathcal{U}_Y, K_A^{(S)}}(z) \leq F_{\mathcal{U}_X, K_A^{(S)}}(z).$$

This formulation captures the core idea of FSD within structured environments, offering a systematic way to assess and compare probabilistic dominance under constraints.

Then, we point out that, for any  $p \in ]0, 1[$ ,

$$Q_{\mathcal{U}_Y, K_A^{(S)}}^-(p) \subseteq Q_{\mathcal{U}_X, K_A^{(S)}}^-(p).$$

The proof of this set inclusion is straightforward from (25).

**Remark 9** As already stated in Sect. 2.3, the parameter  $p \in ]0, 1[$  governs the selectiveness of the lower and upper cone quantile functions. For instance, a higher value of  $p$  leads to a more conservative classification of top-performing alternatives, represented by  $Q_{X, K_A}^-(p)$ . Conversely, a lower value of  $p$  yields a broader selection, which may be preferable when decision-makers want to consider a wider set of potentially acceptable options. Similar reasoning applies to the classification of low-performing alternatives, represented by  $Q_{X, K_A}^+(p)$ .

As discussed in Hamel and Kostner (2024), a DM may wish to select (or exclude) a specific percentage  $\alpha\%$  of best-performing (or poorly performing) alternatives from the entire set. This can be achieved by finding the largest value of  $p$  such that

$$\#\left\{i = 1, \dots, m : x^E(a_i) \in Q_{X, K_A}^-(p)\right\} \geq \frac{m\alpha}{100}.$$

Choosing  $p$  according to this inequality allows the user to select the desired number of top alternatives. A similar approach can be used to exclude the worst  $\alpha\%$  of alternatives.

## 6 Results and Discussion

In this section, we present a case study involving a MCDM problem focused on ranking different portfolios. A financial advisory firm seeks to identify the most suitable portfolios from a set of 21 alternatives, based on three key financial criteria:

- *expected return* ( $\gamma_1$ ): the average return a portfolio is expected to generate;
- *buffer* ( $\gamma_2$ ): measures how much a portfolio's Value-at-Risk (VaR) falls below a predefined maximum acceptable loss. For portfolio  $i$ :

$$\text{buffer}_i = 100 \times \left( \frac{\text{ML}_{\text{accepted}} - \text{VaR}_i}{\text{ML}_{\text{accepted}}} \right),$$

where  $\text{VaR}_i$  denotes the value-at-risk of portfolio  $i$  and  $\text{ML}_{\text{accepted}}$  is the maximum acceptable loss defined by the decision-maker;

- *liquidity* ( $\gamma_3$ ): the ease of converting portfolio assets into cash without significant value loss.

We begin with the case where evaluations are provided by an external expert and the judges' importance vectors are fixed, following the setup in Kostner (2020), extended here to a three-dimensional context. We then explore the effects of introducing uncertainty in either the importance vectors or the criteria evaluations, and finally, we examine the combined impact of both sources of uncertainty on the ranking of alternatives.

### 6.1 Deterministic Criteria Evaluations and Importance Vectors

This study considers 21 portfolio alternatives evaluated across three criteria by an external financial analyst. The evaluations are represented as:

$$X^E(a_i) = \begin{bmatrix} x^E(\gamma_1, a_i) \\ x^E(\gamma_2, a_i) \\ x^E(\gamma_3, a_i) \end{bmatrix} \in \mathbb{R}^3,$$

where  $x^E(\gamma_k, a_i)$  is the evaluation of portfolio  $a_i$  on criterion  $\gamma_k$ . Table 2 reports the evaluations for all alternatives.

The values in Table 2 are percentage-based. Expected return ( $\gamma_1$ ) ranges from 0.9% to 2.9%, buffer ( $\gamma_2$ ) from 0.5% to 5.9%, and liquidity ( $\gamma_3$ ) from 0.5% to 2.7%. Higher values across all criteria are considered preferable.

We consider three judges, each assigning their own importance weights to the criteria:

$$v^1 = \begin{bmatrix} 1.7 \\ 1.2 \\ 1.2 \end{bmatrix}, \quad v^2 = \begin{bmatrix} 1.4 \\ 1.6 \\ 1.0 \end{bmatrix}, \quad v^3 = \begin{bmatrix} 1.2 \\ 1.2 \\ 0.7 \end{bmatrix}. \quad (30)$$

Judge 1 emphasizes expected return, with equal but lower importance on buffer and liquidity. Judge 2 gives highest priority to buffer, reflecting a preference for stability. Judge 3 assigns generally lower weights, especially to liquidity, indicating a conservative style favoring return and downside protection. These differences in preferences shape the resulting rankings.

Using the evaluations and importance vectors, we apply the MCDM framework from Kostner (2020), which combines the individual judge rankings through the cone distribution function to derive a collective ranking that balances all viewpoints.

We compute the *cone distribution function*  $F_{X, K_A}(z)$  and the *scalar distribution functions*  $F_{X, v^j}(z)$  for each judge  $j \in \{1, 2, 3\}$ . The results and rankings are summarized in Table 3. The cone distribution function assigns each alternative a conservative rank by taking the worst-case rank across all feasible directions within the acceptance cone  $K_A$ . In contrast, the scalar distribution functions reflect the individual rankings of each judge.

Figure 6 illustrates, in blue the lower  $K_A$ -quantile  $Q_{X, K_A}^-(p)$  and in light red the upper  $K_A$ -quantile  $Q_{X, K_A}^+(p)$  for four values of  $p$ . These quantiles are computed for the set of assessed alternatives  $X$  (reported in Table 2) and for the acceptance cone  $K_A$  generated by the importance vectors  $v^1, v^2$ , and  $v^3$ .

## 6.2 Uncertainty in Expert Evaluation and Importance Vectors

In this section, we introduce uncertainty in both the evaluations of alternatives and the importance vectors. For illustration, we consider 6 possible perturbed scenarios, each representing potential variations in the assessment of the 21 portfolio alternatives across the three financial criteria. In particular, for any alternative  $a_i$ ,  $i = 1, \dots, m$ , the perturbed scenarios  $X^\kappa(a_i)$ , are defined as

$$X^\kappa(a_i) = X(a_i) + \Delta^\kappa(a_i), \quad \kappa = 1, \dots, 6,$$

**Table 2** Evaluation of 21 alternatives based on expected return ( $\gamma_1$ ), buffer ( $\gamma_2$ ) and liquidity ( $\gamma_3$ ). Higher values are more desirable. A higher buffer indicates greater distance from downside risk, while higher liquidity implies easier asset convertibility without significant loss

$a_i$	$\gamma_1$ (%)	$\gamma_2$ (%)	$\gamma_3$ (%)	$a_i$	$\gamma_1$ (%)	$\gamma_2$ (%)	$\gamma_3$ (%)	$a_i$	$\gamma_1$ (%)	$\gamma_2$ (%)	$\gamma_3$ (%)
$a_1$	2.0	2.5	1.5	$a_8$	2.3	2.0	1.7	$a_{15}$	1.3	1.9	2.0
$a_2$	1.0	3.0	1.9	$a_9$	1.4	2.3	1.5	$a_{16}$	2.1	1.5	1.7
$a_3$	1.8	2.0	2.3	$a_{10}$	0.9	2.5	1.9	$a_{17}$	2.9	4.5	1.2
$a_4$	2.5	1.5	2.2	$a_{11}$	1.5	2.1	2.3	$a_{18}$	2.0	3.5	0.5
$a_5$	2.7	0.8	1.2	$a_{12}$	2.8	1.2	2.2	$a_{19}$	1.3	5.9	0.8
$a_6$	2.2	2.0	2.2	$a_{13}$	2.9	0.5	1.2	$a_{20}$	2.1	2.5	1.7
$a_7$	1.8	1.5	2.0	$a_{14}$	2.0	1.5	2.2	$a_{21}$	2.9	4.5	2.7

where  $\Delta^\kappa(a_i)$  is a point generated according to a uniform distribution within the Euclidean ball centered at 0 of radius  $\delta = 0.15$ . This ensures that each perturbed alternative lies within a bounded neighborhood of the original one. Figure 7 visualizes the uncertainty set of the original evaluations (blue dots) and the simulated scenarios (red dots). The light red spheres depict the uncertainty regions around each original evaluation, reflecting possible deviations due to factors such as data limitations, subjective interpretation, or changing market conditions.

We also consider three scenarios for the importance vectors. Figure 8 shows a graphical representation of the original vectors (red) and their perturbed versions (blue), plotted in the three-dimensional space of expected return, buffer, and liquidity.

We now analyze the effects of introducing uncertainty into the evaluation process, examining how the results vary depending on the chosen modeling approach. By comparing different strategies for handling uncertainty, we assess their influence on the rankings and robustness of the alternatives. To this end, we introduce six ranking methods, each representing a distinct treatment of uncertainty in the evaluations and/or importance vectors, defined as follows:

*Method 1 – No uncertainty* The baseline approach developed by Kostner (2020) assumes no uncertainty in either the evaluations or the importance vectors. The ranking is based on the cone distribution function  $F_{X, K_A}(z)$ , where  $X$  denotes the deterministic evaluations. The acceptance cone  $K_A$  is generated from fixed importance vectors and defines the set of alternatives deemed acceptable.

*Method 2 – Uncertainty in the evaluations* This method introduces uncertainty in the evaluations  $X$  while keeping the importance vectors  $v^j$  (for  $j = 1, 2, 3$ ) deterministic. It captures variation in the performance of alternatives but assumes that the relative importance of criteria remains fixed. Rankings are computed using the cone distribution function  $F_{U_X, K_A}(z)$  from (11), which evaluates the worst-case ranking across the uncertainty set  $U_X$ .

*Method 3 – Uncertainty in importance vectors* Here, the evaluations are deterministic, but the importance vectors are uncertain, reflecting variability in decision-makers' preferences. The ranking is computed via  $F_{X, K_A^{(S)}}(z)$ , defined in (12),

where  $K_A^{(S)}$  is the robust acceptance cone generated from a family of perturbed importance cones (see (7)). This method evaluates alternatives under the most unfavorable weighting scenario.

*Method 4 – Union-based importance vector* In this case, evaluations are deterministic, while the acceptance cone is generated from the union of all uncertain importance vectors. The resulting cone  $K_A^S$  is the intersection of all individual acceptance cones (see (8)), and the ranking is based on  $F_{X, K_A^S}(z)$ . This approach allows for a more inclusive treatment of uncertainty, incorporating all directions that are acceptable in at least one scenario. It provides a different way of incorporating uncertainty in the importance vectors, capturing a broader set of feasible ranking directions.

*Method 5 – Fully robust* This method introduces uncertainty in both evaluations and importance vectors. The ranking is computed using  $F_{U_X, K_A^{(S)}}(z)$ , which

**Table 3** Values of the cone distribution function  $F_{X, K_A}(z)$  and the scalar distribution functions  $F_{X, v^j}(z)$  for each alternative  $z = x^E(a_i)$ 

$a_i$	$F_{X, K_A}(z)$	$F_{X, v_1}(z)$	$F_{X, v_2}(z)$	$F_{X, v_3}(z)$
$a_1$	0.524 (8)	0.571 (10)	0.714 (7)	0.714 (7)
$a_2$	0.381 (12)	0.381 (14)	0.619 (9)	0.476 (12)
$a_3$	0.476 (11)	0.619 (9)	0.476 (12)	0.524 (11)
$a_4$	0.524 (8)	0.762 (6)	0.619 (9)	0.619 (9)
$a_5$	0.095 (17)	0.238 (17)	0.095 (20)	0.095 (20)
$a_6$	0.714 (4)	0.810 (5)	0.762 (6)	0.762 (6)
$a_7$	0.190 (16)	0.286 (16)	0.190 (18)	0.190 (18)
$a_8$	0.571 (6)	0.667 (8)	0.667 (8)	0.667 (8)
$a_9$	0.095 (17)	0.143 (19)	0.286 (16)	0.286 (16)
$a_{10}$	0.048 (19)	0.048 (21)	0.333 (15)	0.238 (17)
$a_{11}$	0.381 (12)	0.429 (13)	0.429 (13)	0.429 (13)
$a_{12}$	0.524 (8)	0.857 (4)	0.524 (11)	0.571 (10)
$a_{13}$	0.048 (19)	0.190 (18)	0.048 (21)	0.048 (21)
$a_{14}$	0.381 (12)	0.476 (12)	0.381 (14)	0.381 (14)
$a_{15}$	0.048 (19)	0.095 (20)	0.143 (19)	0.143 (19)
$a_{16}$	0.238 (15)	0.333 (15)	0.238 (17)	0.333 (15)
$a_{17}$	0.952 (2)	0.952 (2)	0.952 (2)	0.952 (2)
$a_{18}$	0.571 (6)	0.571 (10)	0.857 (4)	0.857 (4)
$a_{19}$	0.905 (3)	0.905 (3)	0.905 (3)	0.905 (3)
$a_{20}$	0.667 (5)	0.714 (7)	0.810 (5)	0.810 (5)
$a_{21}$	1.000 (1)	1.000 (1)	1.000 (1)	1.000 (1)

The corresponding rankings are shown in parentheses

evaluates each alternative across all combinations of uncertain evaluations and weighting scenarios (see (9)). Further details can be found in Sect. 4.

*Method 6 – Union-based importance vectors and uncertainty in evaluations* This method combines uncertainty in evaluations with the inclusive acceptance cone  $K_A^S$  from point 4. An alternative is considered acceptable if it is deemed acceptable in at least one realization of uncertainty. Rankings are determined using  $F_{U_X, K_A^S}(z)$  as in (11).

Table 4 reports the results of the six ranking methods applied to the 21 portfolio alternatives. For each method, the corresponding worst-case CDF value is reported for every alternative, along with its rank in parentheses. This enables a direct comparison of how different approaches to modeling uncertainty in both evaluations and importance vectors affect the stability and reliability of decision outcomes.

The following differences can be observed in the rankings derived from the six methods above. We observe differences in the CDF values when comparing methods that handle uncertainty in the importance vectors differently, i.e., in Method 3 vs. Method 4, or Method 5 vs. Method 6. In both cases, the CDF based on the union-generated cone is consistently “flatter” than the one derived from uncertainty in the importance vectors, meaning that in Method 4 (respectively 6), the number of alternatives sharing the same rank is higher than in Method 3 (respectively 5). This results in a larger set of alternatives that are mutually indifferent and, thus, a less selective ranking process. These trends reveal essential differences in how uncertainty is incorporated into the decision-making process.

We observe a consistent trend: as uncertainty increases, the CDF becomes flatter. This effect is most evident when uncertainty is introduced in both the evaluations and the importance vectors. As the level of uncertainty grows, the model tends to become less decisive in ranking alternatives. This pattern is particularly evident when comparing different approaches:

- $F_{X, K_A}(z)$  vs.  $F_{U_X, K_A}(z)$ , showing the impact of uncertainty in evaluations, with fixed importance vectors.
- $F_{X, K_A}(z)$  vs.  $F_{X, K_A^{(S)}}(z)$ , capturing the effect of uncertain importance vectors with deterministic evaluations.
- $F_{U_X, K_A}(z)$  vs.  $F_{U_X, K_A^{(S)}}(z)$ , showing how ranking is affected when uncertainty in importance vectors is added to evaluation uncertainty.
- $F_{X, K_A^{(S)}}(z)$  vs.  $F_{U_X, K_A^{(S)}}(z)$ , comparing deterministic evaluations to uncertain evaluations when importance vectors are already uncertain.

This case study reinforces the notion that incorporating uncertainty into the decision-making process tends to soften the ranking structure, resulting in a greater number of alternatives receiving similar acceptability scores. Such behavior reflects the reduced discriminative power caused by uncertainty. The results also highlight how different uncertainty-handling approaches influence the robustness and inclusiveness of final rankings.

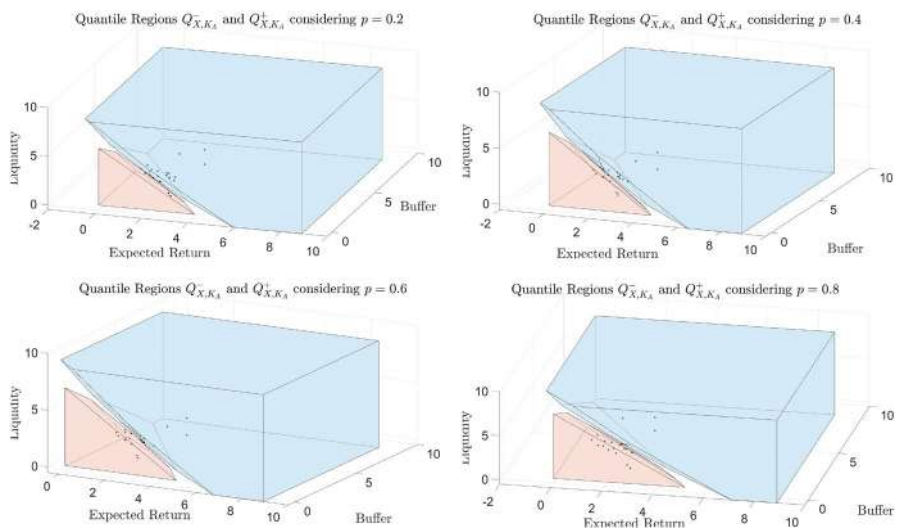


**Fig. 6** In blue the set  $Q_{X,K_A}^-(p)$  and in light red the set  $Q_{X,K_A}^+(p)$  for  $p = 0.2, 0.4, 0.6, 0.8$ , with the importance cone  $K_A$  generated by the judges  $v^1, v^2$ , and  $v^3$

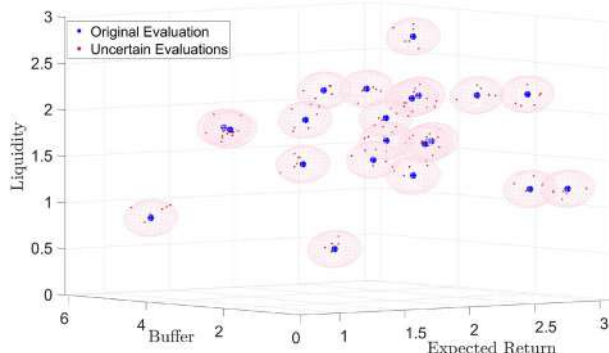


**Fig. 7** Visualization of uncertain evaluations in the three-dimensional criterion space

We now analyse how uncertainty affects the quantile boundaries used to classify alternatives. In particular, we investigate how the lower and upper quantiles of the evaluations change when uncertainty is introduced in both the importance vectors and the evaluation criteria. These quantiles provide insight into the range of potential performance outcomes and help clarify how different sources of uncertainty shape the decision-making process.

In the absence of uncertainty, the evaluations of the alternatives, reported in Table 2, are provided by a single external expert, while the importance vectors, given in Eq. 30, are fixed and determined by three judges. Following the method proposed in Kostner (2020), we compute and plot the upper and lower quantiles for various levels of  $p$ . When uncertainty is introduced, we consider multiple scenarios: Fig. 7

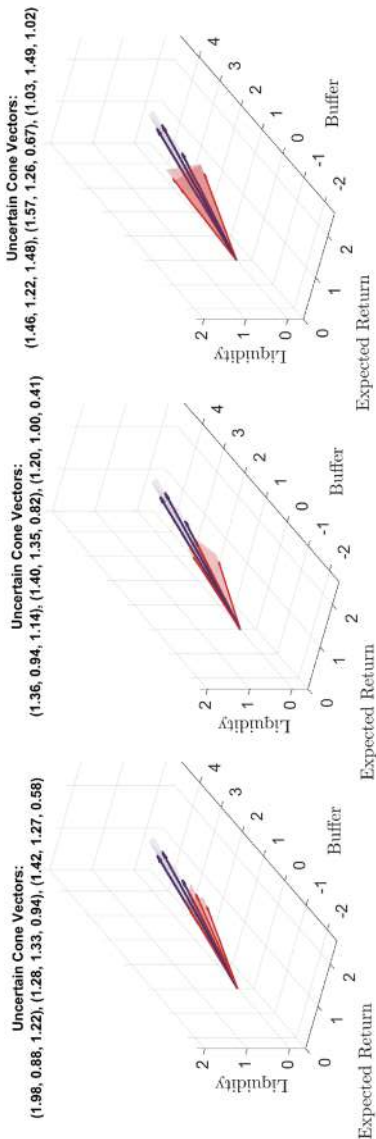


**Fig. 8** Graphical representation of original and uncertain importance vectors across different scenarios

**Table 4** Comparison of different evaluation methods, including uncertainty and robustness considerations

$a_i$	$F_{X, K_A}(z)$	$F_{U_X, K_A}(z)$	$F_{X, K_A^{(S)}}(z)$	$F_{X, K_A^S}(z)$	$F_{U_X, K_A^{(S)}}(z)$	$F_{U_X, K_A^S}(z)$
$a_1$	0.524 (8)	0.524 (6)	0.476 (6)	0.476 (6)	0.476 (6)	0.429 (6)
$a_2$	0.381 (12)	0.333 (12)	0.190 (14)	0.190 (14)	0.190 (12)	0.190 (11)
$a_3$	0.476 (11)	0.476 (7)	0.476 (6)	0.476 (6)	0.429 (7)	0.429 (6)
$a_4$	0.524 (8)	0.476 (7)	0.476 (6)	0.476 (6)	0.429 (7)	0.429 (6)
$a_5$	0.095 (17)	0.048 (16)	0.048 (17)	0.048 (16)	0.048 (16)	0.048 (15)
$a_6$	0.714 (4)	0.571 (5)	0.667 (4)	0.667 (4)	0.524 (5)	0.476 (5)
$a_7$	0.190 (16)	0.048 (16)	0.095 (16)	0.048 (16)	0.048 (16)	0.048 (15)
$a_8$	0.571 (6)	0.429 (10)	0.476 (6)	0.476 (6)	0.429 (7)	0.429 (6)
$a_9$	0.095 (17)	0.048 (16)	0.048 (17)	0.048 (16)	0.048 (16)	0.048 (15)
$a_{10}$	0.048 (19)	0.048 (16)	0.048 (17)	0.048 (16)	0.048 (16)	0.048 (15)
$a_{11}$	0.381 (12)	0.333 (12)	0.333 (12)	0.333 (12)	0.190 (12)	0.190 (11)
$a_{12}$	0.524 (8)	0.429 (10)	0.429 (10)	0.429 (10)	0.429 (7)	0.429 (6)
$a_{13}$	0.048 (19)	0.048 (16)	0.048 (17)	0.048 (16)	0.048 (16)	0.048 (15)
$a_{14}$	0.381 (12)	0.238 (14)	0.333 (12)	0.333 (12)	0.190 (12)	0.143 (14)
$a_{15}$	0.048 (19)	0.048 (16)	0.048 (17)	0.048 (16)	0.048 (16)	0.048 (15)
$a_{16}$	0.238 (15)	0.143 (15)	0.143 (15)	0.095 (15)	0.095 (15)	0.048 (15)
$a_{17}$	0.952 (2)	0.905 (2)	0.905 (2)	0.905 (2)	0.905 (2)	0.905 (2)
$a_{18}$	0.571 (6)	0.476 (7)	0.381 (11)	0.381 (11)	0.238 (11)	0.190 (11)
$a_{19}$	0.905 (3)	0.905 (2)	0.762 (3)	0.762 (3)	0.762 (3)	0.762 (3)
$a_{20}$	0.667 (5)	0.667 (4)	0.667 (4)	0.667 (4)	0.619 (4)	0.619 (4)
$a_{21}$	1.000 (1)	1.000 (1)	1.000 (1)	1.000 (1)	1.000 (1)	1.000 (1)

Values are presented with their respective ranks in parentheses

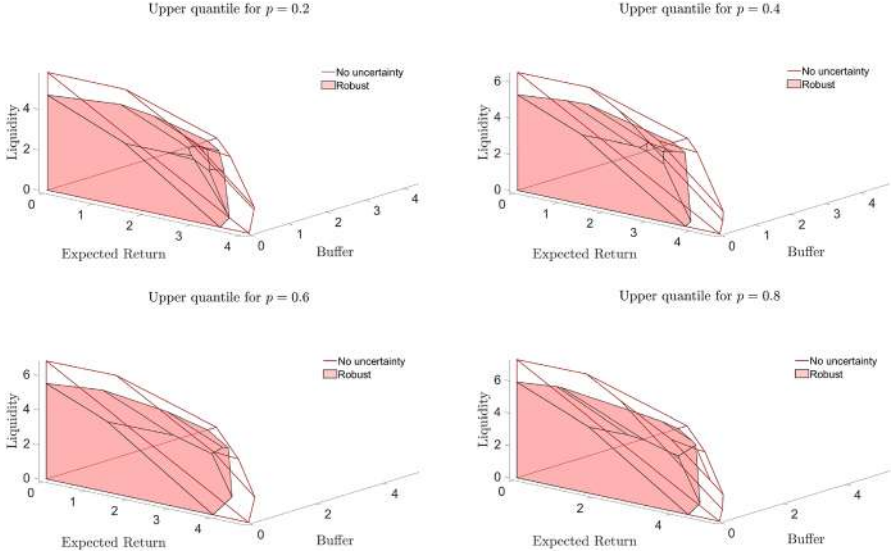


**Fig. 9** For four different levels of  $p = \{0.2, 0.4, 0.6, 0.8\}$ , each subplot illustrates the upper quantile  $Q_{X,K_A}^+$  in the absence of uncertainty, represented by a transparent region outlined only by red boundary lines. The robust upper quantile  $Q_{U_X,K_A^{(S)}}^+$ , which accounts for uncertainty, is shown in light red.

Uncertainty is incorporated in both the evaluation criteria and importance vectors

illustrates scenarios for the evaluations, and Fig. 8 shows those for the importance vectors. Our analysis follows the robust quantile methodology outlined in Sect. 4.2.

Figures 9 and 10 show the impact of uncertainty on the upper and lower quantiles, respectively. These robust quantiles incorporate uncertainty in both the evaluation criteria and the importance vectors. Each figure presents results for four values of  $p$ , specifically  $p = \{0.2, 0.4, 0.6, 0.8\}$ , allowing us to assess how uncertainty influences the range of possible outcomes.

In Fig. 9, the transparent region outlined by red boundary lines represents the upper quantile  $Q_{X,K_A}^+$  under no uncertainty. The robust upper quantile  $Q_{U_X,K_A^{(S)}}^+$ , which accounts for uncertainty, is shown as a light red shaded region (refer to (24)). The difference between these regions highlights the effect of uncertainty on identifying the worst-performing alternatives. For all values of  $p$ , the robust upper quantile shifts downward, implying that uncertainty leads to a stricter classification of poorly performing alternatives. This suggests that alternatives previously viewed as poor performers may be reassessed as more acceptable under uncertainty, due to the model's consideration of potential variability in evaluations.

Similarly, Fig. 10 illustrates the impact of uncertainty on the lower quantile for four different levels of  $p = \{0.2, 0.4, 0.6, 0.8\}$ . Each subplot compares the non-robust lower quantile  $Q_{X,K_A}^-$ , depicted as a transparent region outlined by blue boundary lines, with the robust lower  $K_A^{(S)}$ -quantile function  $Q_{U_X,K_A^{(S)}}^-$ , shown as a light

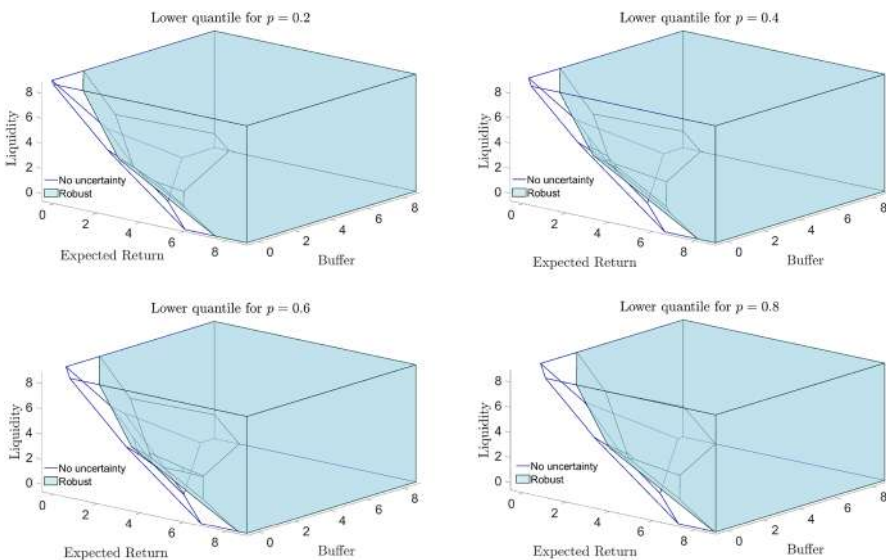


**Fig. 10** For four different levels of  $p = \{0.2, 0.4, 0.6, 0.8\}$ , each subplot illustrates the lower quantile  $Q_{X,K_A}^-$  in the absence of uncertainty, represented by a transparent region outlined only by blue boundary lines. The robust lower quantile  $Q_{U_X,K_A^{(S)}}^-$  is shown as a light blue shaded region. Uncertainty is incorporated in both the evaluation criteria and importance vectors

blue shaded area (see (24)). The results show that as  $p$  increases, the lower quantile becomes more selective, retaining only the most favorable alternatives. Conversely, for smaller values of  $p$ , the lower quantile expands, including a broader set of alternatives as potential best performers. Across all values of  $p$ , the robust lower quantile consistently includes fewer alternatives than the non-robust version, emphasizing the more stringent selection process induced by uncertainty. This behavior reflects the increasing conservatism of the evaluation process under uncertainty, making it more challenging for alternatives to consistently qualify among the best.

Tables 5 and 6 compare the alternatives included in the lower and upper quantiles across different values of  $p$ , under both the non-uncertainty and robust approaches. For higher values of  $p$  (e.g.,  $p = 0.6, 0.8$ ), the lower quantile becomes more selective, identifying only top-performing alternatives (Table 5). As  $p$  decreases, the lower quantile expands, reflecting a less conservative evaluation. Across all  $p$  levels, the robust lower quantile includes fewer alternatives with respect to the baseline approach, highlighting a more cautious selection process under uncertainty. Alternatives  $a_{17}, a_{19}$ , and  $a_{21}$  consistently appear as robust top performers. These results are consistent with the trends observed in Fig. 10.

For the upper quantile, smaller  $p$  values (e.g.,  $p = 0.2$ ) lead to a more restrictive classification of poorly performing alternatives (Table 6). As  $p$  increases, the quantile expands, incorporating more alternatives that might be at risk of lower evaluations. This behavior aligns with the cone quantile framework described in Kostner (2020), where increasing  $p$  leads to a broader set of alternatives classified within

**Table 5** Alternatives included in the lower quantile for different levels of  $p$ , comparing the non-uncertainty and robust approaches

$Q_{X,K_A}^-$	$Q_{\mathcal{U}_X,K_A^{(S)}}^-$	$Q_{X,K_A}^-$	$Q_{\mathcal{U}_X,K_A^{(S)}}^-$	$Q_{X,K_A}^-$	$Q_{\mathcal{U}_X,K_A^{(S)}}^-$	$Q_{X,K_A}^-$	$Q_{\mathcal{U}_X,K_A^{(S)}}^-$
0.2	0.4	0.6	0.8				
$a_1$	$a_1$	$a_1$	$a_1$				
$a_2$				$a_1$			
$a_3$	$a_3$	$a_3$			$a_3$		
$a_4$	$a_4$	$a_4$			$a_4$		
$a_6$	$a_6$	$a_6$			$a_6$		
$a_8$	$a_8$	$a_8$			$a_8$		
$a_{11}$	$a_{11}$	$a_{11}$					
$a_{12}$	$a_{12}$	$a_{12}$					
$a_{14}$	$a_{14}$						
$a_{16}$							
$a_{17}$	$a_{17}$	$a_{17}$					
$a_{18}$	$a_{18}$	$a_{18}$					
$a_{19}$	$a_{19}$	$a_{19}$					
$a_{20}$	$a_{20}$	$a_{20}$					
$a_{21}$	$a_{21}$	$a_{21}$					
				$a_{17}$	$a_{17}$	$a_{17}$	$a_{17}$
				$a_{18}$			
				$a_{19}$	$a_{19}$	$a_{19}$	$a_{19}$
				$a_{20}$	$a_{20}$	$a_{20}$	$a_{20}$
				$a_{21}$	$a_{21}$	$a_{21}$	$a_{21}$

**Table 6** Alternatives included in the upper quantile for different levels of  $p$ , comparing the non-uncertainty and robust approaches

$Q_{X, K_A}^+$	$Q_{\mathcal{U}_{X, K_A}(S)}^+$	$Q_{X, K_A}^+$	$Q_{\mathcal{U}_{X, K_A}(S)}^+$	$Q_{\mathcal{U}_{X, K_A}(S)}^+$	$Q_{X, K_A}^+$	$Q_{\mathcal{U}_{X, K_A}(S)}^+$
0.2						
		0.4		0.6		0.8
$a_5$		$a_5$	$a_5$	$a_5$	$a_5$	$a_5$
	$a_7$		$a_7$		$a_7$	$a_7$
$a_9$		$a_9$	$a_9$	$a_9$	$a_9$	$a_9$
$a_{10}$		$a_{10}$	$a_{10}$	$a_{10}$	$a_{10}$	$a_{10}$
				$a_{11}$	$a_{11}$	$a_{11}$
$a_{13}$			$a_{13}$	$a_{13}$	$a_{13}$	$a_{13}$
				$a_{14}$	$a_{14}$	$a_{14}$
$a_{15}$		$a_{15}$	$a_{15}$	$a_{15}$	$a_{15}$	$a_{15}$
	$a_{16}$		$a_{16}$	$a_{16}$	$a_{16}$	$a_{16}$

the quantile. The robust set-quantile is generally more selective than the set-quantile without uncertainty, as the former approach includes fewer alternatives classified as poor-performing. This reflects the fact that under the robust approach, the selection process accounts for worst-case evaluations, making it stricter in identifying truly poor-performing alternatives. Finally, alternatives such as  $a_5$ ,  $a_7$ , and  $a_{15}$  appear consistently, suggesting they are persistently among the lowest-ranked options, regardless of the levels of conservatism considered. These findings align with the patterns shown in Fig. 9.

These results highlight how uncertainty influences both the upper and lower quantiles of the evaluations. In particular, incorporating uncertainty shifts the quantile boundaries, which can significantly affect the ranking of alternatives. These variations underscore the importance of accounting for uncertainty to ensure a more robust and reliable decision-making process.

## 7 Conclusions

This paper proposes a robust quantile-based method for ranking alternatives under uncertainty, extending the framework introduced by Kostner (2020). Our approach incorporates uncertainty in both the evaluation criteria and the importance vectors, resulting in a more comprehensive and risk-aware decision-making process. By analyzing worst-case cumulative distribution functions (CDFs), we obtained quantile regions that characterize the performance of alternatives across different levels of conservatism.

The methodology allows for flexible modeling of uncertainty, supporting both traditional deterministic settings and robust scenarios. In particular, we examined six alternative strategies for incorporating uncertainty, distinguishing between approaches that use the intersection or union of acceptance cones when aggregating uncertain importance vectors. This comparison revealed that the way uncertainty is treated has a significant impact on the resulting rankings.

The case study confirms key trends: intersection-based methods (e.g., using  $K_A^S$ ) yield steeper CDFs and more selective rankings, while union-based methods (e.g., using  $K_A^{(S)}$ ) produce flatter CDFs and broader classifications. Increasing uncertainty consistently leads to flatter CDFs and less discriminative rankings. This trend demonstrates how uncertainty influences the robustness and inclusiveness of the decision-making outcomes. It also underscores the importance of carefully selecting the uncertainty model based on the decision-maker's risk preferences.

Overall, the proposed framework provides a structured and interpretable approach for incorporating uncertainty into multi-criteria ranking problems. It enables decision-makers to balance robustness and inclusivity while accounting for variability in both data and preference structures. Future research could investigate the integration of this framework with machine-learning-based methods for estimating uncertainty, compare its performance with alternative robust MCDM approaches, or explore its applicability to complex decision environments such as financial risk control, health-

care resource allocation, urban development, and ecological management, where decision robustness is critical.

**Acknowledgements** The authors acknowledge the financial support of Fondazione Cariplo through the project “MultiLocal” (Grant No. 2022-1548). They also gratefully acknowledge INdAM–GNAMPA for supporting their research activities.

**Open Access** This article is licensed under a Creative Commons Attribution 4.0 International License, which permits use, sharing, adaptation, distribution and reproduction in any medium or format, as long as you give appropriate credit to the original author(s) and the source, provide a link to the Creative Commons licence, and indicate if changes were made. The images or other third party material in this article are included in the article’s Creative Commons licence, unless indicated otherwise in a credit line to the material. If material is not included in the article’s Creative Commons licence and your intended use is not permitted by statutory regulation or exceeds the permitted use, you will need to obtain permission directly from the copyright holder. To view a copy of this licence, visit <http://creativecommons.org/licenses/by/4.0/>.

## References

- Bellman RE, Zadeh LA (1970) Decision-making in a fuzzy environment. *Manage Sci* 17(4):141
- Belton V, Stewart TJ (2002) Multiple criteria decision analysis: an integrated approach. Springer, Boston, MA. <https://doi.org/10.1007/978-1-4615-1495-4>
- Brans JP, Vincke P (1985) A preference ranking organisation method: The Promethee method for MCDM. *Manage Sci* 31(6):647–656
- Buckley J (1984) The multiple judge, multiple criteria ranking problem: a fuzzy set approach. *Fuzzy Sets Syst* 13(1):25–37
- Buckley JJ (1985) Fuzzy hierarchical analysis. *Fuzzy Sets Syst* 17(3):233–247
- Buckley JJ (1985) Ranking alternatives using fuzzy numbers. *Fuzzy Sets Syst* 15(1):21–31
- Carlsson C (1982) Tackling an MCDM-problem with the help of some results from fuzzy set theory. *Eur J Oper Res* 10(3):270–281
- Corrente S, Figueira JR, Greco S (2014) The SMAA-PROMETHEE method. *Eur J Oper Res* 239(2):514–522
- Danielson M, Ekenberg L (2017) A robustness study of state-of-the-art surrogate weights for MCDM. *Group Decis Negot* 26(4):677–691
- Dias LC, Freire F, Geldermann J (2019) Perspectives on multi-criteria decision analysis and life-cycle assessment. In: New perspectives in multiple criteria decision making: innovative applications and case studies, pp 315–329. Springer, Cham. [https://doi.org/10.1007/978-3-030-11482-4\\_12](https://doi.org/10.1007/978-3-030-11482-4_12)
- Figueira J, Greco S, Ehrgott M (2016) Multiple criteria decision analysis: state of the art surveys. Springer, New York
- Fu C, Chang W (2024) A Markov chain-based group consensus method with unknown parameters. *Group Decision and Negotiation*, 1–30
- Grabisch M (1996) The application of fuzzy integrals in multicriteria decision making. *Eur J Oper Res* 89(3):445–456
- Hamel AH, Kostner D (2024) Multi-weight ranking for multi-criteria decision making. *Neural Comput Appl*, 1–13
- Hamel AH, Heyde F (2010) Duality for set-valued measures of risk. *SIAM J Financial Math* 1(1):66–95
- Hamel AH, Kostner D (2018) Cone distribution functions and quantiles for multivariate random variables. *J Multivar Anal* 167:97–113
- Kostner D (2020) Multi-criteria decision making via multivariate quantiles. *Math Methods Oper Res* 91(1):73–88
- Lahdelma R, Salminen P (2010) Stochastic multicriteria acceptability analysis (SMAA). In: Ehrgott M, Figueira JR, Greco S (eds) Trends in multiple criteria decision analysis. Springer, Berlin, pp 321–354
- Lahdelma R, Hokkanen J, Salminen P (1998) SMAA - Stochastic multiobjective acceptability analysis. *Eur J Oper Res* 106(1):137–143

- Liu Y (2024) Risk based weight determination in multiple criteria decision making. *Group Decision and Negotiation*, 1–36
- Mareschal B, Brans JP, Vincke P (1984) Promethee: A new family of outranking methods in multicriteria analysis. Technical report, ULB–Université Libre de Bruxelles
- Opricovic S, Tzeng G-H (2004) Compromise solution by MCDM methods: a comparative analysis of VIKOR and TOPSIS. *Eur J Oper Res* 156(2):445–455
- Pajamasmaa J, Miettinen K, Silvennoinen J (2024) Group decision making in multiobjective optimization: a systematic literature review. *Group Decision and Negotiation*, 1–43
- Rockafellar RT (1970) Convex analysis. Princeton University Press, Princeton
- Rowley HV, Peters GM, Lundie S, Moore SJ (2012) Aggregating sustainability indicators: beyond the weighted sum. *J Environ Manage* 111:24–33. <https://doi.org/10.1016/j.jenvman.2012.05.004>
- Roy B (1968) Classement et choix en présence de points de vue multiples. *Revue française d'informatique et de recherche opérationnelle* 2(8):57–75
- Saaty TL (1980) The analytic hierarchy process (AHP). *J Oper Res Soc* 41(11):1073–1076
- Vahdani B, Hadipour H (2011) Extension of the ELECTRE method based on interval-valued fuzzy sets. *Soft Comput* 15:569–579
- Zhang H, Ji Y, Qu S, Li H, Huang R (2022) The robust minimum cost consensus model with risk aversion. *Inf Sci* 587:283–299
- Zhu K, Qu S, Ji Y, Ma Y (2024) Distributionally robust chance constrained maximum expert consensus model with incomplete information on uncertain cost. *Group Decision Negotiation*, 1–41

**Publisher's Note** Springer Nature remains neutral with regard to jurisdictional claims in published maps and institutional affiliations.